A Study on Image Change Detection Methods for Multiple Images of the Same Scene Acquired by a Mobile Camera

Guntur Tanjung

School of Mechanical Engineering

The University of Adelaide

South Australia 5005

Australia

A thesis submitted in fulfilment of the requirements

for the degree of Doctor of Philosophy in

Mechanical Engineering

on the 12th October 2009

CHAPTER 10

EXPERIMENTAL RESULTS AND DISCUSSION

Experimental results and discussion are presented in Chapter 10. Section 10.1 presents a third fuzzy inference system developed in this research in calculating latest possible percentages as significant changes. Section 10.2 presents experimental results produced by the complete change detection method by displaying estimated locations and possible percentages of significant changes in every input image based on information of objects in its changed mask. Section 10.3 discusses these experimental results in order to evaluate performance of the change detection method. Concluding remarks are presented in Section 10.4.

10.1 Third Fuzzy Inference System (FIS3)

Prior to display estimated locations and possible percentage values of significant changes on every input image, latest possible percentage values of objects in every changed mask have to calculate again since possible percentage values produced by the FIS1 and FIS2 tend to have same possible percentage values. When every object in a changed mask has a same possible percentage values, operators in a control room will have a difficulty to decide which significant change that needs an urgent attention or just disregards it. Thus, a third fuzzy inference system (FIS3) is developed in this research in order to compute latest possible percentage values of objects in every changed mask. The FIS3 will produce different possible percentage values of objects in every changed mask. Moreover, important information of each object in a changed mask such as its centroid position and x_width value is also extracted.

The summary of the FIS3 is depicted in Table 10.1 and 10.2, below. Area, y_width, x_width, and *AbsDiffLF* of each object in a changed mask are used as inputs into the FIS3.

Table 10.1 An overview of the FIS3 including its inputs, outputs, and fuzzy rules. a, b, c and d denote Area, y_width, x_width, and $AbsDiffLF$. O symbolizes Probabilityaschange

No	Fuzzy Rules
1	(a == small) & (b == small) & (c == small) & (d == few) ⇒ (O = medium)
2	(a == average) & (b == small) & (c == small) & (d == few) ⇒ (O = medium)
3	(a == large) & (b == large) & (c == large) & (d == considerable) ⇒ (O = very_high)
4	(a == large) & (b == small) & (c == large) & (d == many) ⇒ (O = very_high)
5	(a == large) & (b == large) & (c == small) & (d == many) ⇒ (O = very_high)
6	(a == average) & (b == small) & (c == large) & (d == many) ⇒ (O = high)
7	(a == average) & (b == large) & (c == small) & (d == many) ⇒ (O = high)
8	(a == average) & (b == large) & (c == small) & (d == few) ⇒ (O = medium)
9	(a == average) & (b == small) & (c == large) & (d == few) ⇒ (O = medium)
10	(a == large) & (b == large) & (c == large) & (d == many) ⇒ (O = very_high)
11	(a == large) & (b == large) & (c == large) & (d == considerable) ⇒ (O = very_high)
12	(a == small) & (b == large) & (c == small) & (d == few) ⇒ (O = medium)
13	(a == small) & (b == small) & (c == large) & (d == few) ⇒ (O = medium)

As depicted in Table 10.1 above, the FIS3 has four inputs (Area, y_width, x_width and *AbsDiffLF*), one output (Probabilityaschange) and 13 fuzzy rules. Area is interpreted as {Small, Average, Large} and y_width and x_width are interpreted as {Small, Large}. *AbsDiffLF* is denoted as {Few, Many, Considerable}. The output is decoded as {Medium, High, Very_High}.

The *AbsDiffLF* variable is the 4^{th} fuzzy input of the FIS3. It stands for absolute difference of local features. The following steps are used to generate a *AbsDiffLF* value.

For every object in the HDS1_II,

1. Extract bounding box parameters of the object including upper left corner of the object bounding box in X and Y axes, width and height of the object,
2. Based on these parameters, crop a template from its ROI2_RI (T_1) and a template from its ROI2_II (T_2),
3. Extract local features from T_1 (LF_1) and from T_2 (LF_2) by using the SIFT operator,
4. Calculate an absolute value of subtraction of LF_1 and LF_2 and the absolute difference of LF_1 and LF2 is assigned to the *AbsDiffLF* variable.

The FIS3 has the same principal with the FIS1 and FIS2 since the FIS3 is a Mamdani's fuzzy inference system. The detail of how a Mamdani's fuzzy inference system works is presented in Section 7.3.2 of Chapter 7. Areas, widths, heights and absolute difference values of local features extracted from objects in every changed mask are utilized as fuzzy inputs by the FIS3 in deciding their possible percentage values. The more an object in a changed mask has such the fuzzy inputs, the more the object has a higher possible percentage value, vice versa.

Triangular membership functions (trimfs) were used for all inputs and the output. Parameters of the triangular membership functions are summarized in Table 10.2, below.

Table 10.2 Summarization of triangular membership function parameters

	trimfs	**Parameters**
Area	Small	[0 3500 7000]
	Average	[7000 12000 20000]
	Large	[20000 40000 80000]
y_width	Small	[0 50 120]
	Large	[120 300 500]
x_width	Small	[0 50 120]
	Large	[120 300 500]
AbsDiffLF	Few	[0 15 50]
	Many	[50 80 150]
	Considerable	[150 320 800]
O	Medium	[49 55 60]
	High	[60 70 85]
	Very_High	[85 90 100]

10.2 Experimental Results

This section has three sub-sections. The first, second and third sub-sections will present detecting results of input images captured by a mobile camera from the first, second and third outdoor scenes.

10.2.1 First Outdoor Scene

Figs. 10.1 (a), 10.1 (b) and 10.1 (c) depict estimated locations and latest possible percentage values of significant changes detected by the complete change detection method from the ROI2_II-1, ROI2_II-5 and ROI2_II-9.

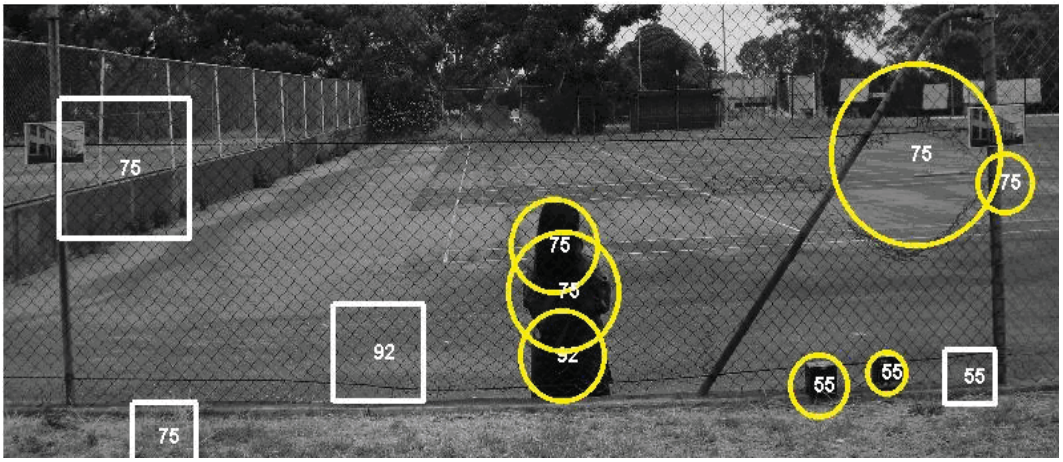

(a)

(b)

(c)

Fig. 10.1 Estimated locations and latest possible percentage values of significant changes detected by the change detection method from the ROI2_II-1 (a), ROI2_II-5 (b) and ROI2_II-9 (c)

As seen in Figs. 10.1 (a), 10.1 (b) and 10.1 (c), significant changes are displayed in two different forms and colours. A white square form indicates an object disappearing and a yellow circle form denotes an object appearing including attached objects in front of fence wires and breaches in the integrity of fence wires. The intruder is often located several times since it is detected in both first and second algorithms. Although the change detection method can detect all significant changes, several unimportant changes observably appear as well. The unimportant changes are often detected on the grass, a wall's surface of fence wires and left and right posts of fence wires. Possible percentage values have a range from 60 to 100. A region with a 92 % denotes that the region has a high alert attention and operators in a control room have to check the region.

Figs. 10.2 (a), 10.2 (b) and 10.3 (c) depict detection results produced by the change detection method from the ROI2_II-2, ROI2_II-6 and ROI2_II-10.

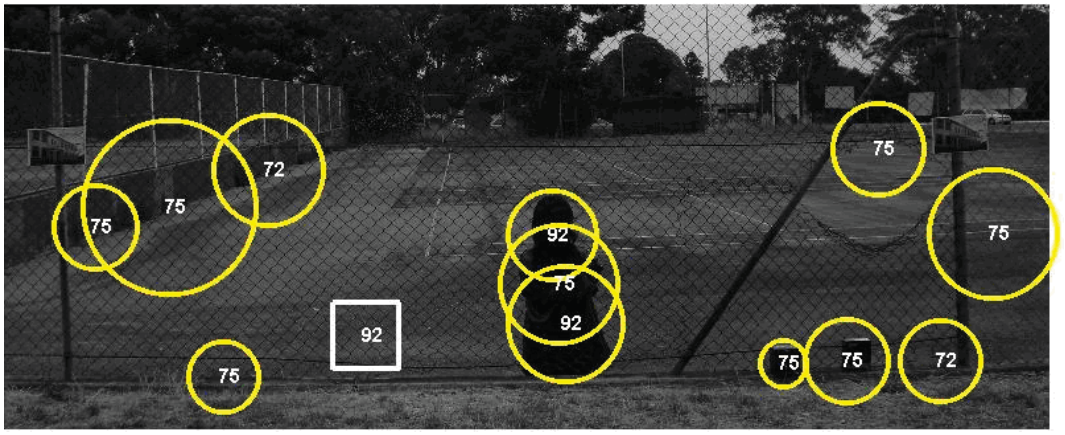

(a)

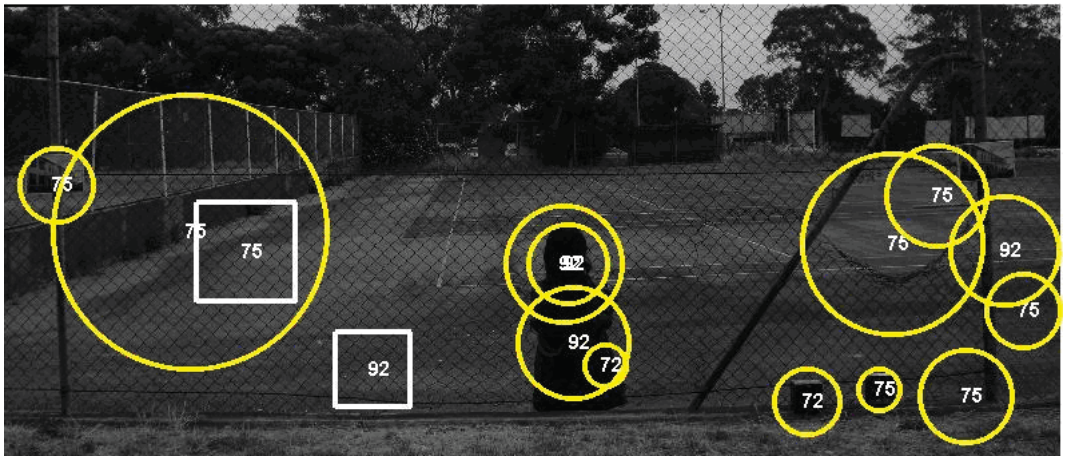

(b)

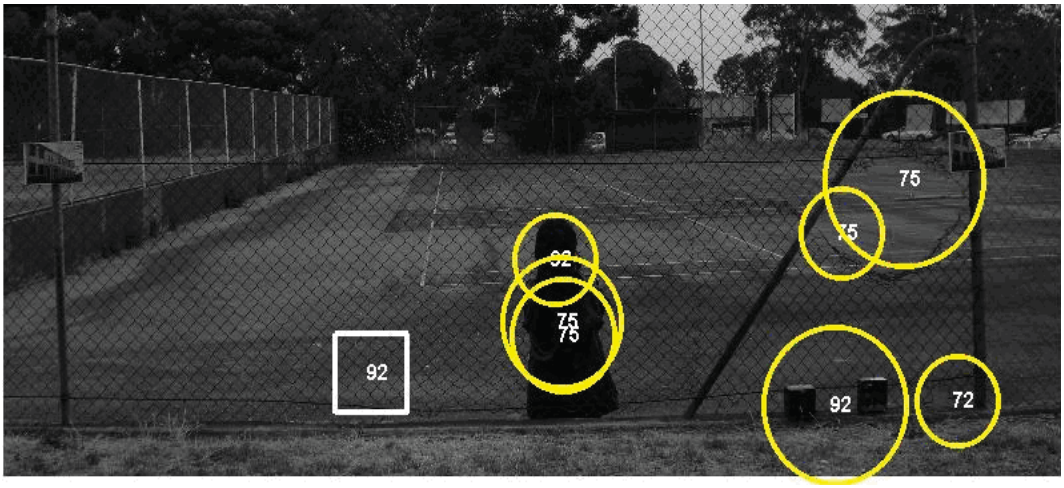

(c)

Fig. 10.2 Detection results provided by the change detection method from the ROI2_II-2 (a), ROI2_II-6 (b) and ROI2_II-10 (c)

As can be seen in Figs 10.2 (a), 10.2 (b) and 10.2 (c), all significant changes are correctly detected by the change detection method. However, more unimportant changes observably appear as well especially in Figs. 10.2 (a) and 10.2 (b). These unimportant changes are mainly caused by background clutter such as trees and a wall's surface of fence wires.

Estimated locations and possible percentages extracted by the change detection method from the ROI2_II-3, ROI2_II-7 and ROI2_II-11 are depicted in Figs. 10.3 (a), 10.3 (b) and 10.3 (c).

(a)

(b)

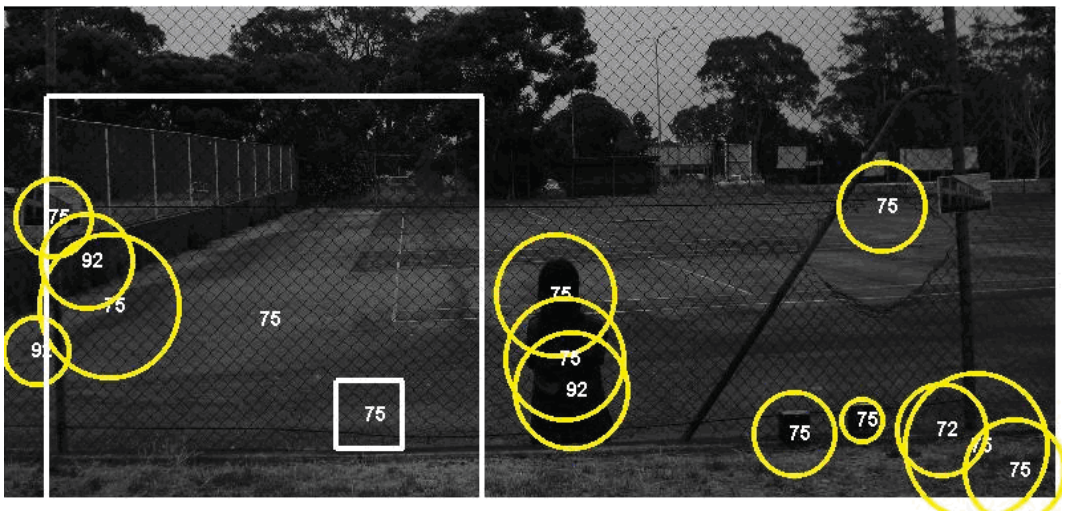

(c)

Fig. 10.3 Estimated locations and possible percentages of significant changes produced by the change detection method from the ROI2_II-3 (a), ROI2_II-7 (b) and ROI2_II-11 (c)

As seen in Figs. 10.3 (a), 10.3 (b) and 10.3 (c), all significant changes are correctly detected by the change detection method from the ROI2_II-3, ROI2_II-7 and ROI2_II-11. However, many unimportant changes observably appear in Fig. 10.3 (c). These unimportant changes are mainly caused by (1) non-uniform illumination that occurs on edges of fence wires, (2) background clutter such trees and a wall's surface of fence wires and (3) left and right posts of fence wires.

Figs. 10.4 (a), 10.4 (b) and 10.4 (c) depict detection results generated by the change detection method from the ROI2_II-4, ROI2_II-8 and ROI2_II-12.

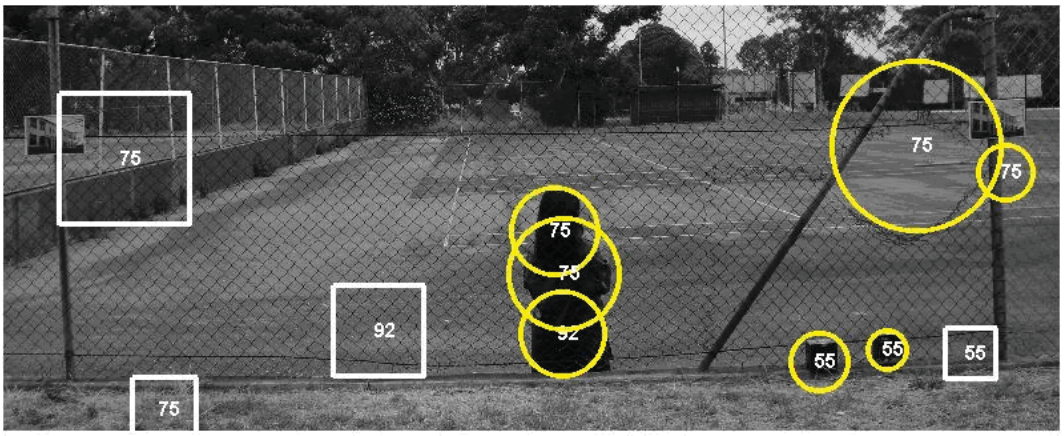

(a)

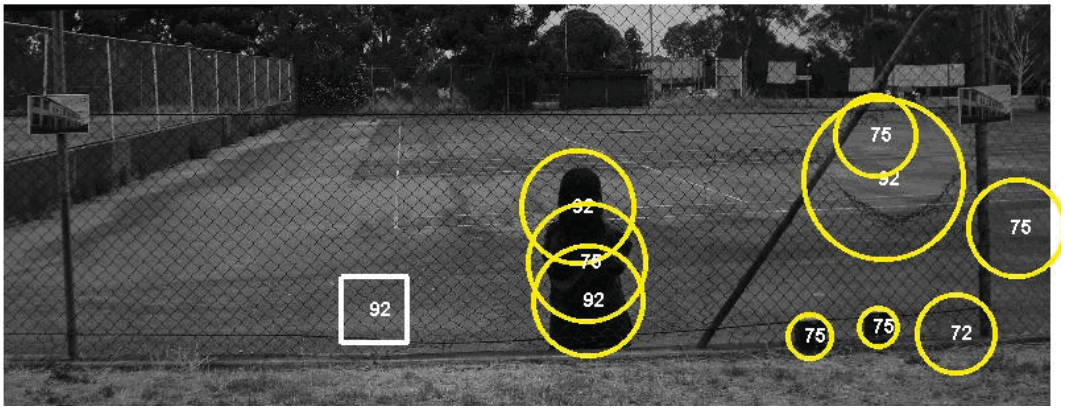

(b)

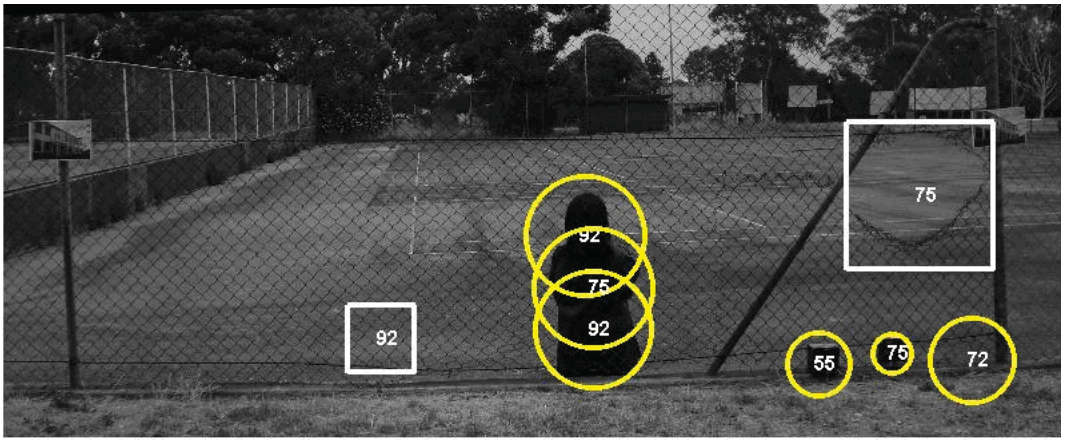

(c)

Fig. 10.4 Detection results produced by the change detection method from the ROI2_II-4 (a), ROI2_II-8 (b) and ROI2_II-12 (c)

As can be seen in Figs. 10.4 (a), 10.4 (b) and 10.4 (c), all significant changes are correctly located by the change detection method. An unimportant change is also

detected by the change detection method in Fig. 10.4 (b). The intruder is located three times since it is detected in both first and second algorithms.

10.2.2 Second Outdoor Scene

In this sub-section, new multiple outdoor images of the same scene captured by a mobile camera from the second outdoor scene are represented. The outdoor change detection method is then applied to the new multiple outdoor images. Detection results (i.e., changed masks and depicting locations of changes) of the new multiple outdoor images are presented in this sub-section as well.

10.2.2.1 Reference and Input Images

13 new images were captured by a mobile camera on 15th of September 2009 from the second outdoor scene containing fence wires including one new reference image and 12 new input images. Table 10.3 depicts a summarization of camera positions and times when capturing 13 new images.

Table 10.3 Summarization of camera positions and times when capturing 13 new images from the second outdoor scene

Images	**Positions (X, Y, $\Delta\theta_z$)**	**Times (hr:mn:sc) PM**
Reference Image	(0, 0, 0)	01:15:34
Input Image 1 (II-1)	(+20, +20, -15)	01:42:20
Input Image 5 (II-5)	(0, +20, 0)	01:42:38
Input Image 9 (II-9)	(+10, +10, -10)	01:43:14
Input Image 2 (II-2)	(+20, -20, -15)	02:16:08
Input Image 6 (II-6)	(+20, 0, -10)	02:16:28
Input Image 10 (II-10)	(+10, -10, -10)	02:16:54
Input Image 3 (II-3)	(-20, -20, +15)	02:44:28
Input Image 7 (II-7)	(0, -20, 0)	02:44:38
Input Image 11 (II-11)	(-10, -10, +10)	02:44:46
Input Image 4 (II-4)	(-20, +20, +15)	03:16:06
Input Image 8 (II-8)	(-20, 0, +10)	03:16:22
Input Image 12 (II-12)	(-10, +10, +10)	03:16:34

As depicted in Table 10.3, the reference image was taken at 01:15:34 PM and the II-1, II-5 and II-9 were taken 27 minutes after capturing the reference image. The

II-1, II-5 and II-9 were captured at slightly different times in simulating that the mobile camera could probably be in one of these positions in the real time application. The II-2, II-6 and II-10 were captured 32 minutes after capturing the previous input images and 59 minutes after capturing the reference image. 28 minutes after capturing the II-2, II-6 and II-10, the II-3, II-7 and II-11 were captured. The II-4, II-8 and II-12 were acquired 28 minutes after capturing the II-3, II-7 and II-11 and around two hours after capturing the reference image.

Fig. 10.5 depicts the reference image captured from the second outdoor scene.

Fig. 10.5 The reference image taken from the second outdoor scene

As seen in Fig. 10.5, the second outdoor scene contains fence wires including left and right posts of the wire fence. Two artificial templates are attached on left and right posts of the wire fence and a school bag is placed behind fence wires.

The following Figs. depict 12 input images captured by a mobile camera from the second outdoor scene.

(a)

(b)

(c)

Fig. 10.6 The II-1 (a), II-5 (b) and II-9 (c) captured from the second outdoor scene

(a)

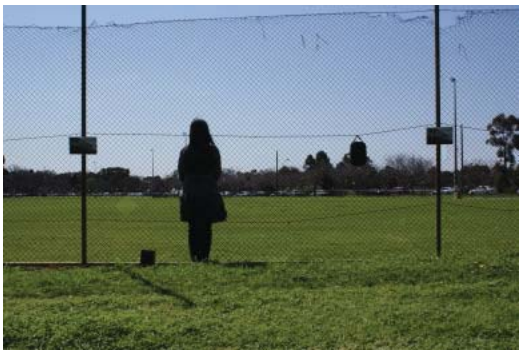

(b)

(c)

Fig. 10.7 The II-2 (a), II-6 (b) and II-10 (c) taken from the second outdoor scene

(a)

(b)

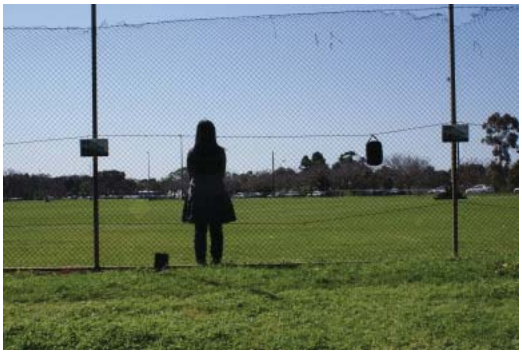

(c)

Fig. 10.8 The II-3 (a), II-7 (b) and II-11 (c) taken from the second outdoor scene

(a)

(b)

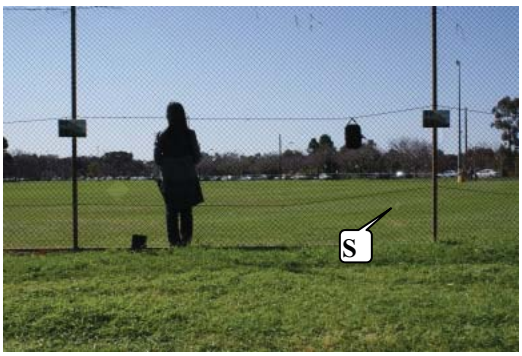

(c)

Fig. 10.9 The II-4 (a), II-8 (b) and II-12 (c) taken from the second outdoor scene

As seen in Figs. 10.6, 10.7, 10.8 and 10.9, a school bag has disappeared and an intruder has appeared behind fence wires. A small box and a small bag have been attached in front of fence wires. Moreover, a medium breach and a small breach, indicated by the S symbol in Fig. 10.9 (c) above, have appeared in the integrity of fence wires. Fig. 10.10, below, depicts an enlargement image of the small breach in the integrity of fence wires.

Fig. 10.10 The small breach that appears in the integrity of fence wires

10.2.2.2 Changed Masks

The outdoor change detection method must be able to detect and locate these significant changes (i.e., absence and presence of a school bag and an intruder behind fence wires, attached objects in front of fence wires and breaches in the integrity of fence wires) while reducing unimportant changes caused by camera motion, illumination variation, background clutter, thinness of fence wires and non-uniform illumination that occurs across fence wires. Next, the new reference image and 12 input images are applied to the outdoor change detection method.

The change detection method is composed by two distinctive algorithms. The first algorithm is used only to detect and locate presence and absence of objects behind fence wires. The second algorithm is utilized only to detect and locate breaches in the integrity of and attached objects in front of fence wires. The following Figs. depict changed masks provided by the first algorithm.

(a) (b)

(c)

Fig. 10.11 The CHM1_II-1 (a), CHM1_II-5 (b) and CHM1_II-9 (c)

(a)

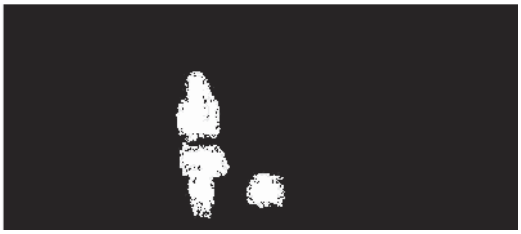

(b)

(c)

Fig. 10.12 The CHM1_II-2 (a), CHM1_II-6 (b) and CHM1_II-10 (c)

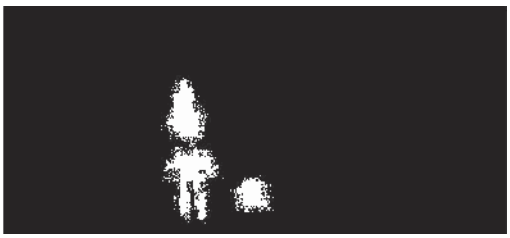

(a)

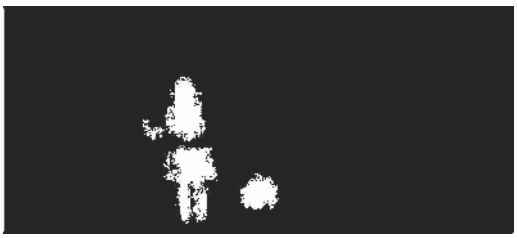

(b)

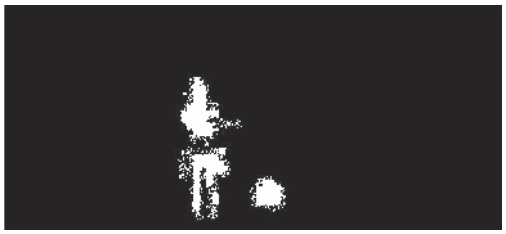

(c)

Fig. 10.13 The CHM1_II-3 (a), CHM1_II-7 (b) and CHM1_II-11 (c)

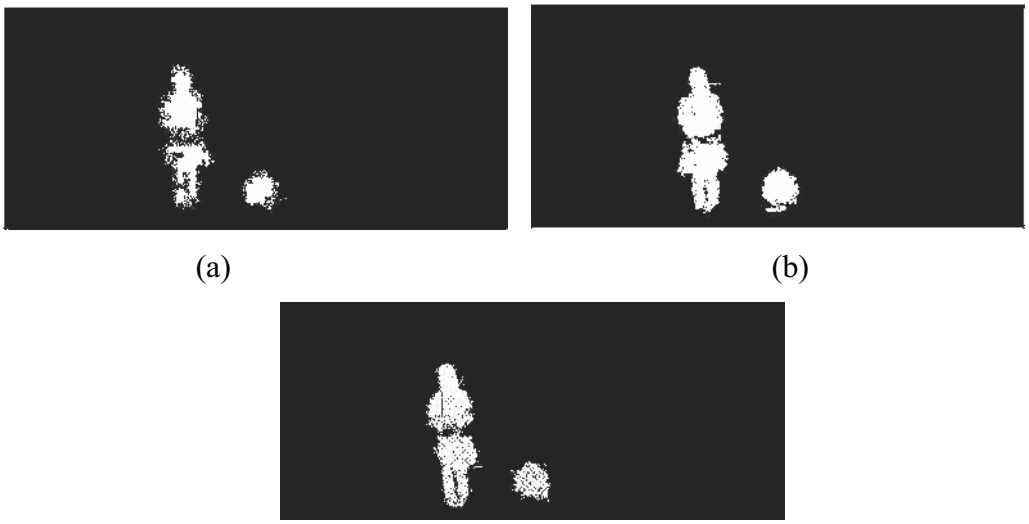

(a) (b)

(c)

Fig. 10.14 The CHM1_II-4 (a), CHM1_II-8 (b) and CHM1_II-12 (c)

As seen in Figs. 10.11, 10.12, 11.13 and 11.14, disappearing of a school bag and appearing of an intruder behind fence wires have been detected by the first algorithm. The intruder has often been divided into two separated objects as a consequence of background clutter of the second outdoor scene. Moreover, both objects are close enough to their original contours and sizes.

The following Figs. depict changed masks produced by the second algorithm.

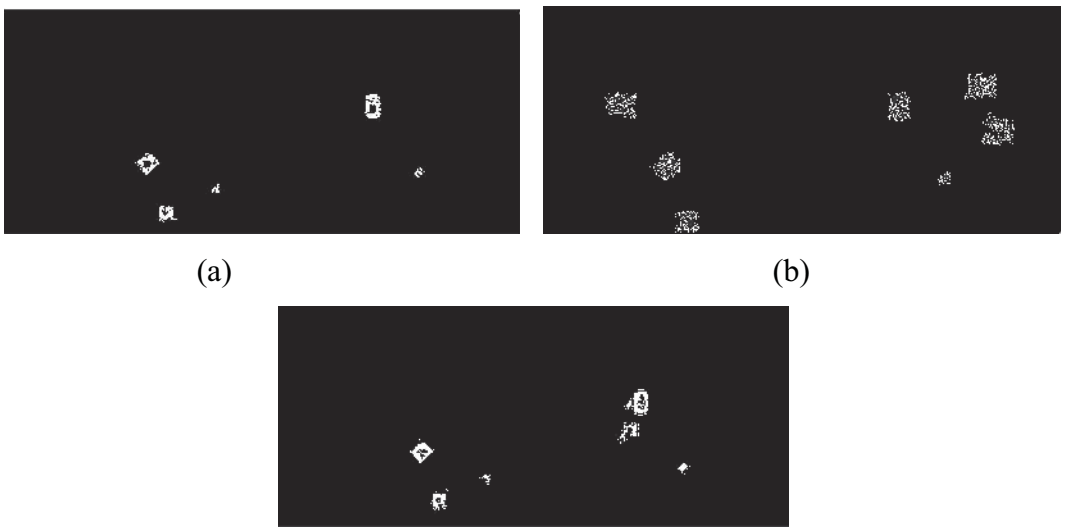

(a) (b)

(c)

Fig. 10.15 The CHM2_II-1 (a), CHM2_II-5 (b) and CHM2_II-9 (c)

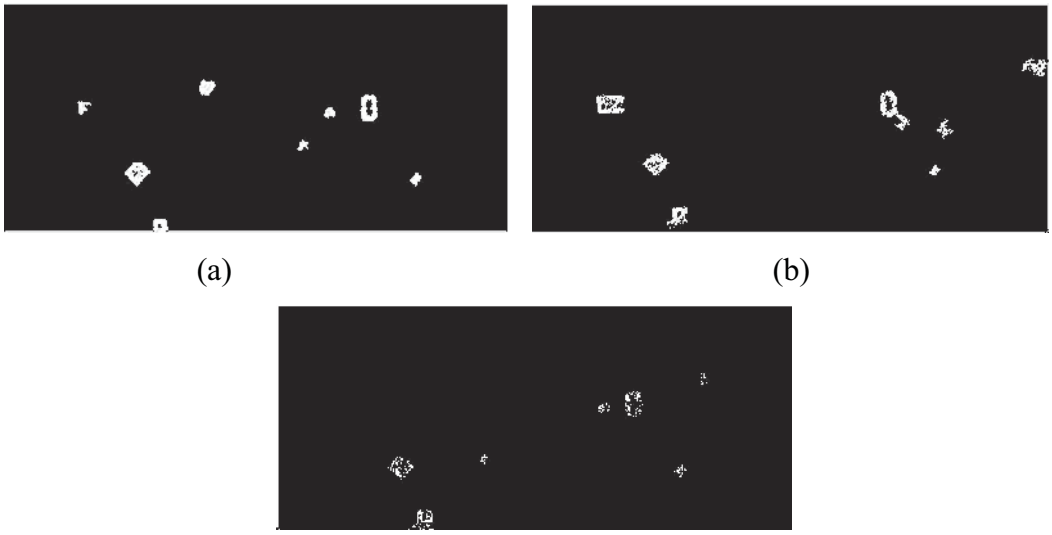

(a) (b)

(c)

Fig. 10.16 The CHM2_II-2 (a), CHM2_II-6 (b) and CHM2_II-10 (c)

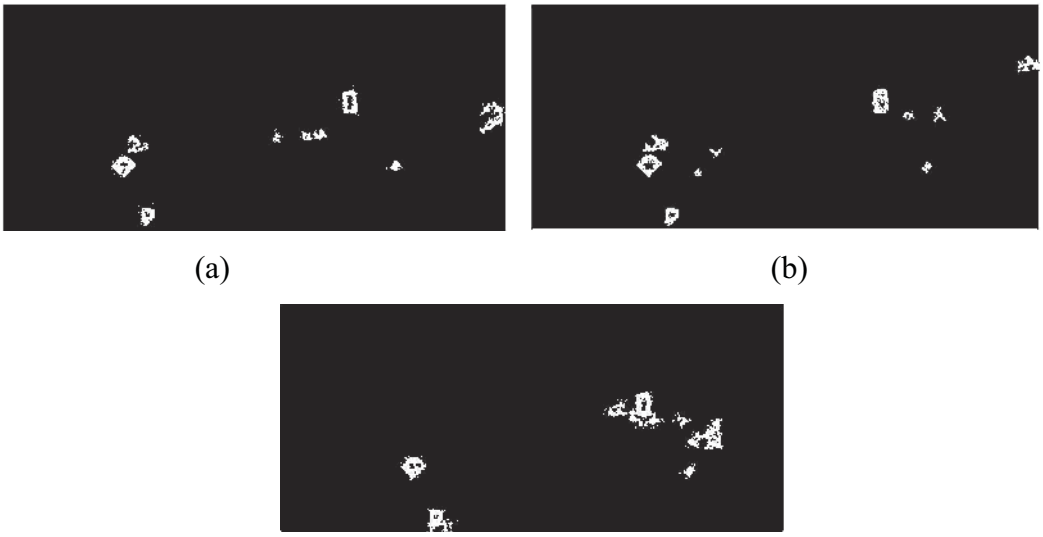

(a) (b)

(c)

Fig. 10.17 The CHM2_II-3 (a), CHM2_II-7 (b) and CHM2_II-11 (c)

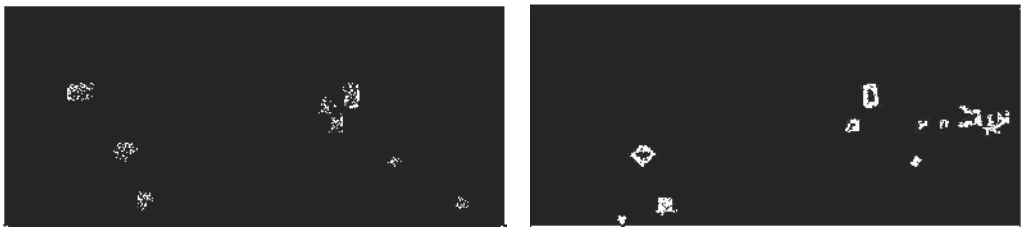

(a) (b)

(c)

Fig. 10.18 The CHM2_II-4 (a), CHM2_II-8 (b) and CHM2_II-12 (c)

As seen in Figs. 10.15, 10.16, 10.17 and 10.18, two breaches and two attached objects have been detected by the second algorithm. However, several unimportant changes have been detected by the second algorithm as well. The unimportant changes are very complicated to be prevented since they are often close enough to size and contour of the small breach.

10.2.2.3 Locations of Changes

Next estimated locations and latest possible percentages of significant changes are depicted on every registered input image using based on information of objects in changed masks provided by the first and second algorithms. The following Figs. depict estimated locations and possible percentages of significant changes on registered input images.

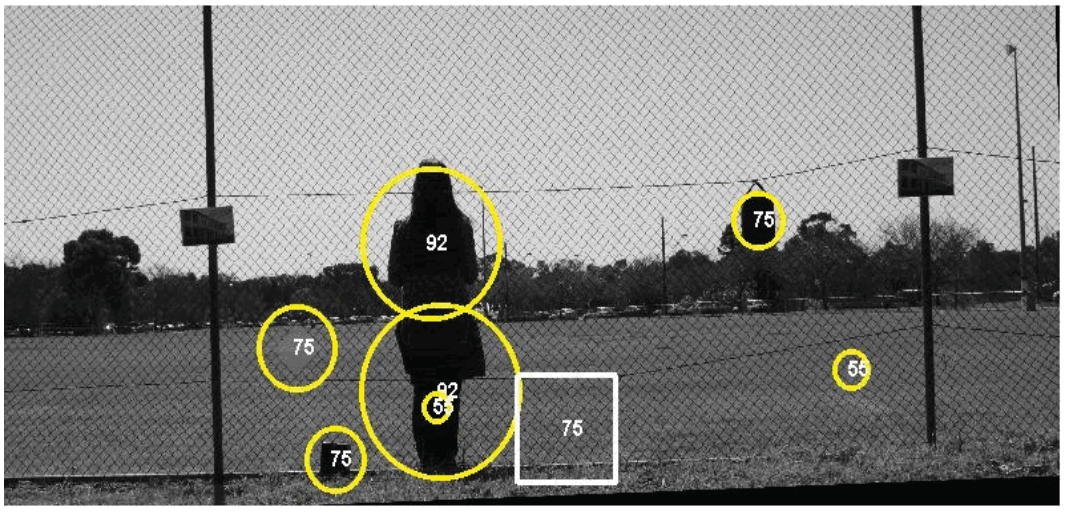

(a)

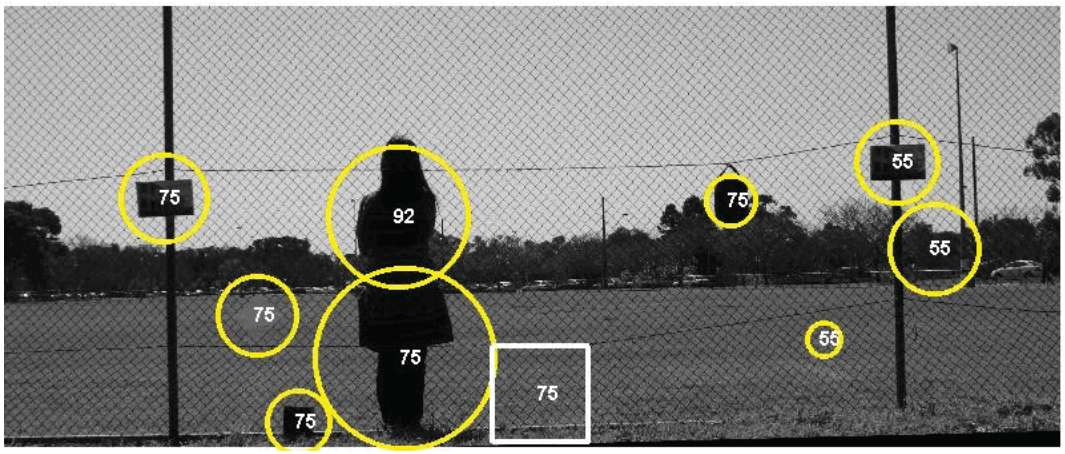

(b)

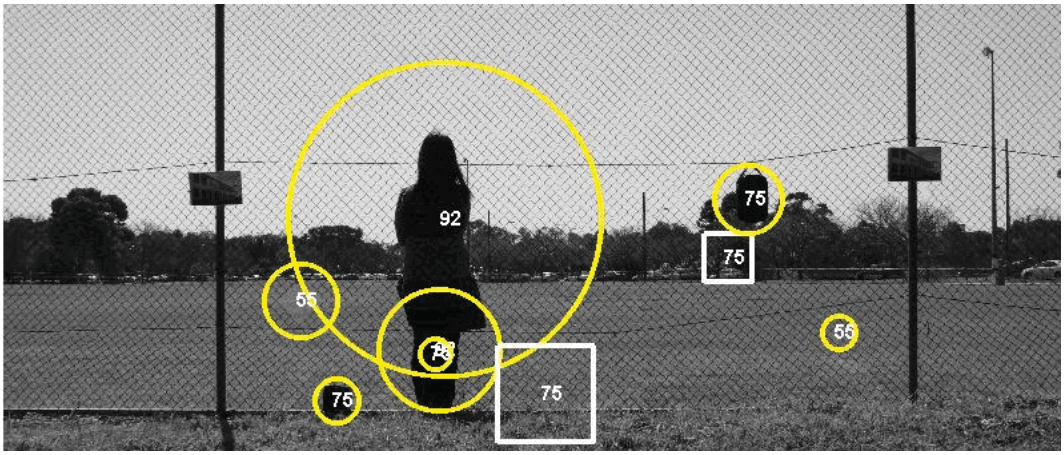

(c)

Fig. 10.19 Estimated locations and possible percentages of significant changes provided by the outdoor change detection method from the ROI2_II-1 (a), ROI2_II-5 (b) and ROI2_II-9 (c)

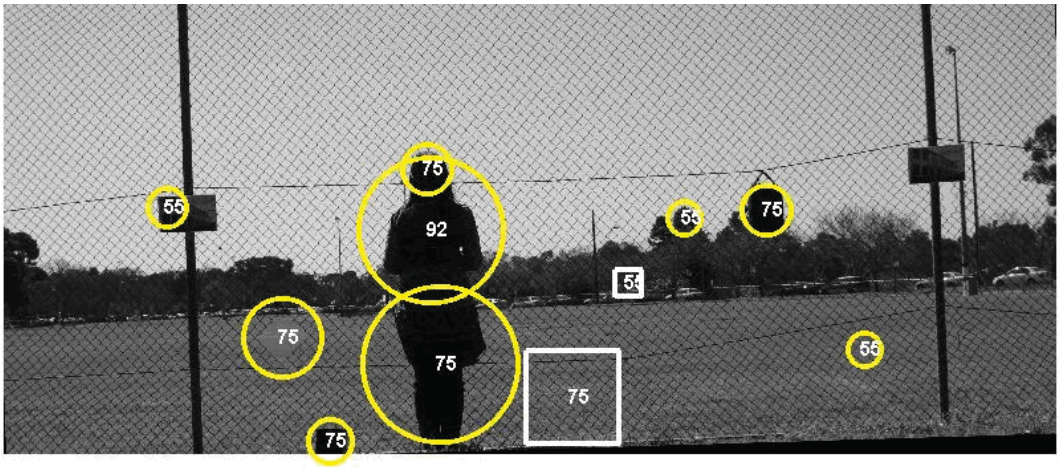

(a)

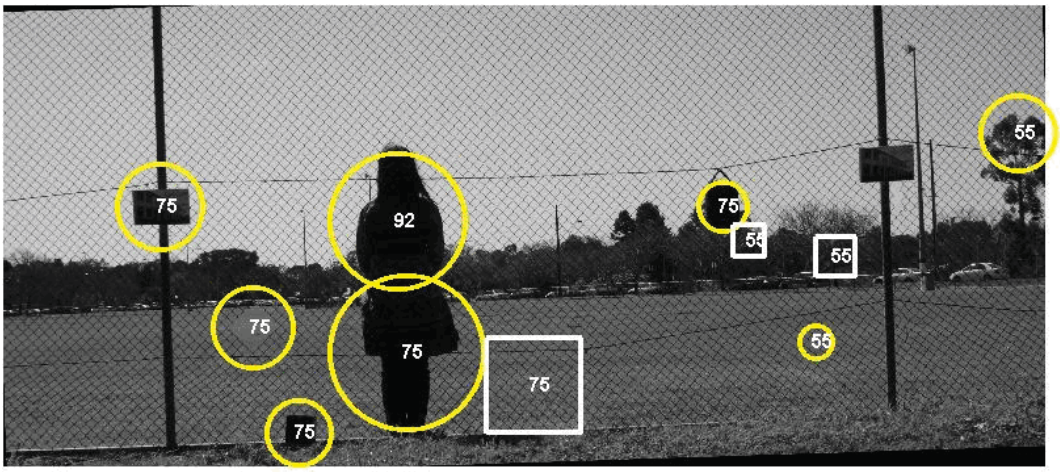

(b)

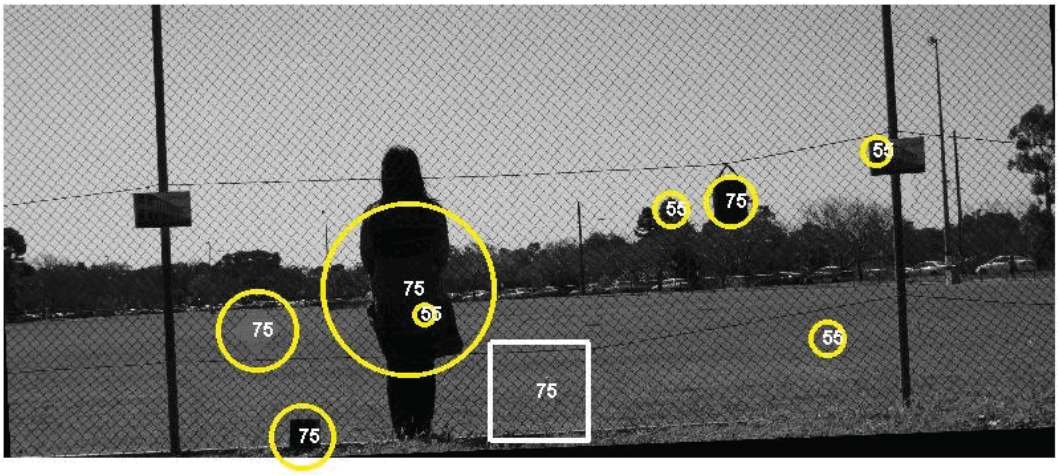

(c)

Fig. 10.20 Estimated locations and possible percentages of significant changes provided by the outdoor change detection method from the ROI2_II-2 (a), ROI2_II-6 (b) and ROI2_II-10 (c)

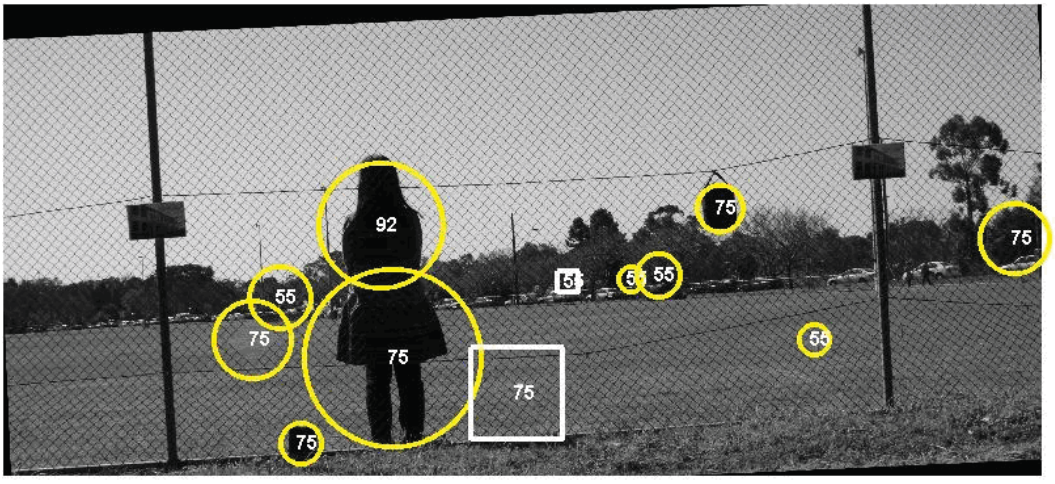

(a)

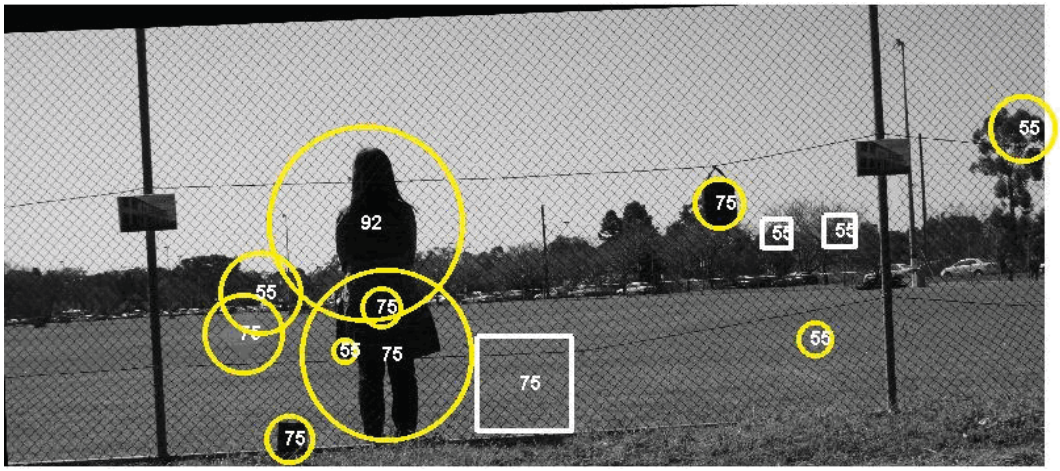

(b)

(c)

Fig. 10.21 Estimated locations and possible percentages of significant changes provided by the outdoor change detection method from the ROI2_II-3 (a), ROI2_II-7 (b) and ROI2_II-11 (c)

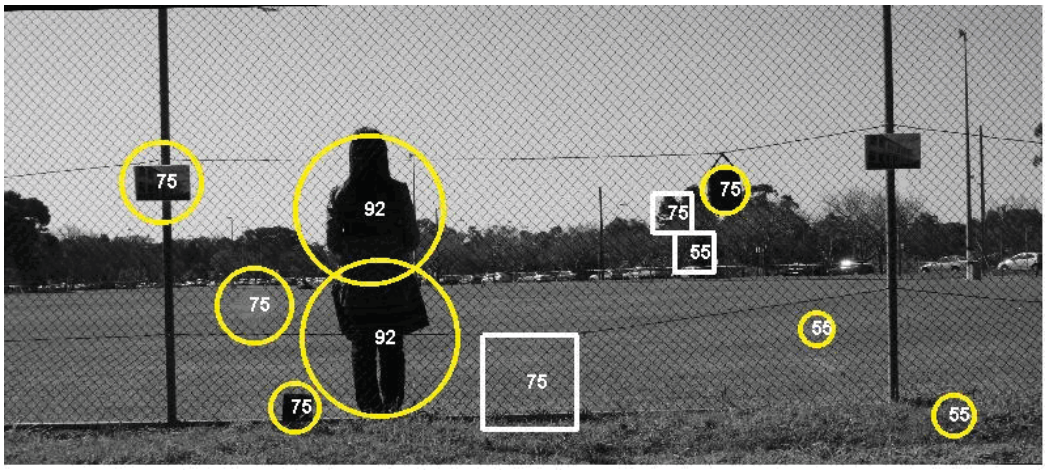

(a)

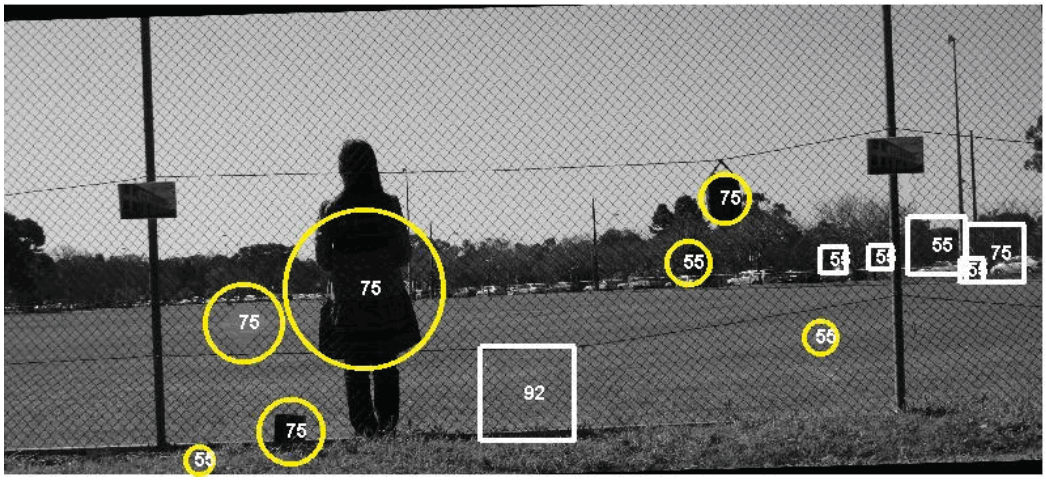

(b)

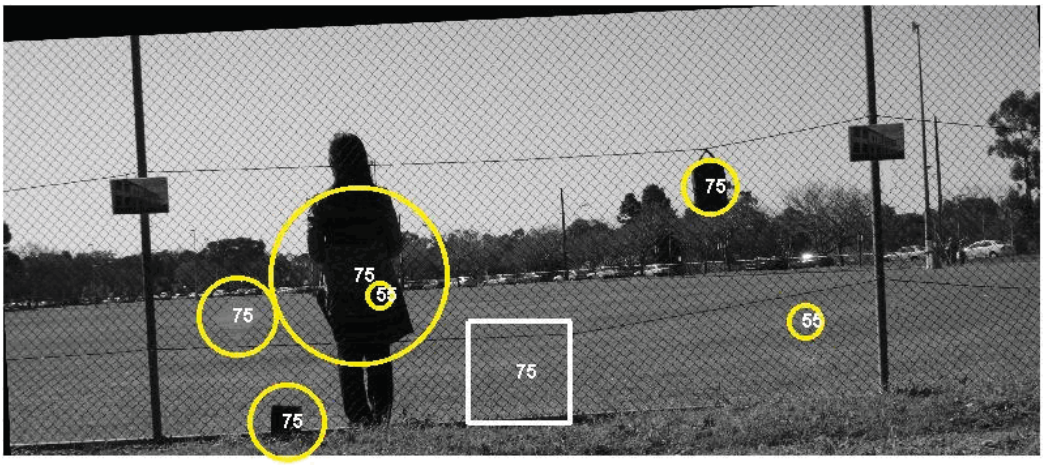

(c)

Fig. 10.22 Estimated locations and possible percentages of significant changes provided by the outdoor change detection method from the ROI2_II-4 (a), ROI2_II-8 (b) and ROI2_II-12 (c)

As seen in Figs. 10.19, 10.20, 10.21 and 10.22, all significant changes such as appearing and disappearing of an intruder and a school bag behind fence wires, two attached objects in front of fence wires and two medium and small breaches in the integrity of fence wires have been detected and located correctly by the outdoor change detection method. Possible percentages of these significant changes are high in the range of 75 – 92 except possible percentage of the small breach is 55. At the same time, the outdoor change detection method has also detected several unimportant changes. Possible percentages of these unimportant changes are often in the range of 55 – 75.

10.2.3 Third Outdoor Scene

In this sub-section, new multiple outdoor images of the same scene captured by a mobile camera from the third outdoor scene are represented. The outdoor change detection method is then applied to the new multiple outdoor images. Detection results (i.e., changed masks and depicting locations of changes) of the new multiple outdoor images are presented in this sub-section as well.

10.2.3.1 Reference and Input Images

13 new images were captured by a mobile camera on 27th of September 2009 from the third outdoor scene containing fence wires including one new reference image and 12 new input images. Table 10.4 depicts a summarization of camera positions and times when capturing 13 new images.

Table 10.4 Summarization of camera positions and times when capturing 13 new images from the third outdoor scene

Images	**Positions (X, Y, $\Delta\theta_z$)**	**Times (hr:mn:sc)**
Reference Image	(0, 0, 0)	11:13:36 AM
Input Image 1 (II-1)	(+20, +20, -15)	12:09:58 PM
Input Image 5 (II-5)	(0, +20, 0)	12:10:08 PM
Input Image 9 (II-9)	(+10, +10, -10)	12:10:20 PM
Input Image 2 (II-2)	(+20, -20, -15)	02:04:46 PM
Input Image 6 (II-6)	(+20, 0, -10)	02:05:00 PM
Input Image 10 (II-10)	(+10, -10, -10)	02:05:40 PM
Input Image 3 (II-3)	(-20, -20, +15)	03:58:12 PM
Input Image 7 (II-7)	(0, -20, 0)	03:58:20 PM
Input Image 11 (II-11)	(-10, -10, +10)	03:58:28 PM
Input Image 4 (II-4)	(-20, +20, +15)	05:45:04 PM
Input Image 8 (II-8)	(-20, 0, +10)	05:45:14 PM
Input Image 12 (II-12)	(-10, +10, +10)	05:45:28 PM

As depicted in Table 10.4, the reference image was taken at 11:13:36 AM and the II-1, II-5 and II-9 were taken 56 minutes after capturing the reference image. The II-1, II-5 and II-9 were captured at slightly different times in simulating that the mobile camera could probably be in one of these positions in the real time application. The II-2, II-6 and II-10 were captured one hour and 54 minutes after

capturing the previous input images and two hours and 52 minutes after capturing the reference image. One hour and 53 minutes after capturing the II-2, II-6 and II-10, the II-3, II-7 and II-11 were captured. The II-4, II-8 and II-12 were acquired one hour and 43 minutes after capturing the II-3, II-7 and II-11 and around six hours and 43 minutes after capturing the reference image.

Fig. 10.23 depicts the reference image captured from the third outdoor scene.

Fig. 10.23 The reference image taken from the third outdoor scene

As seen in Fig. 10.23, the third outdoor scene contains fence wires including left and right posts of the wire fence. Two artificial templates are attached on left and right posts of the wire fence and an intruder appears behind fence wires.

The following Figs. depict 12 input images captured by a mobile camera from the third outdoor scene.

(a)

(b)

(c)

Fig. 10.24 The II-1 (a), II-5 (b) and II-9 (c) captured from the third outdoor scene

(a)

(b)

(c)

Fig. 10.25 The II-2 (a), II-6 (b) and II-10 (c) taken from the third outdoor scene

(a)

(b)

(c)

Fig. 10.26 The II-3 (a), II-7 (b) and II-11 (c) taken from the third outdoor scene

(a)

(b)

(c)

Fig. 10.27 The II-4 (a), II-8 (b) and II-12 (c) taken from the third outdoor scene

As seen in Figs. 10.24, 10.25, 10.26 and 10.27, the intruder has disappeared and a school bag has appeared behind fence wires. A small box and a small bag have been attached in front of fence wires. Moreover, a medium breach has appeared in the integrity of fence wires.

10.2.3.2 Changed Masks

The outdoor change detection method must be able to detect and locate these significant changes (i.e., absence and presence of an intruder and a school bag behind fence wires, attached objects in front of fence wires and a medium breach in the integrity of fence wires) while reducing unimportant changes caused by camera motion, illumination variation, background clutter, thinness of fence wires and non-uniform illumination that occurs across fence wires. Next, the new reference image and 12 input images are applied to the outdoor change detection method.

The following Figs. depict changed masks provided by the first algorithm.

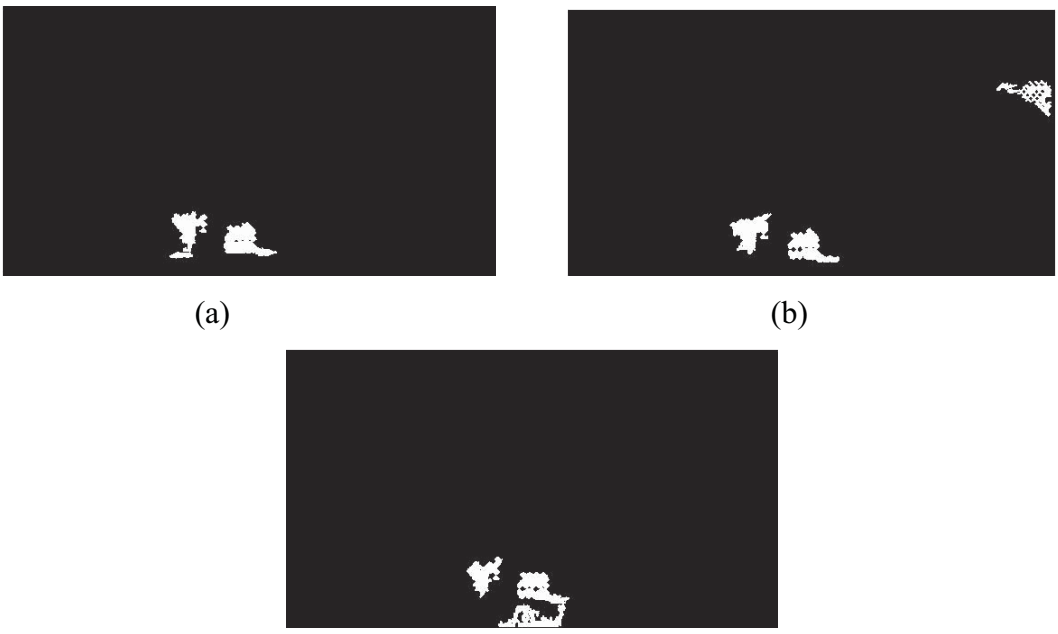

(a) (b)

(c)

Fig. 10.28 The CHM1_II-1 (a), CHM1_II-5 (b) and CHM1_II-9 (c)

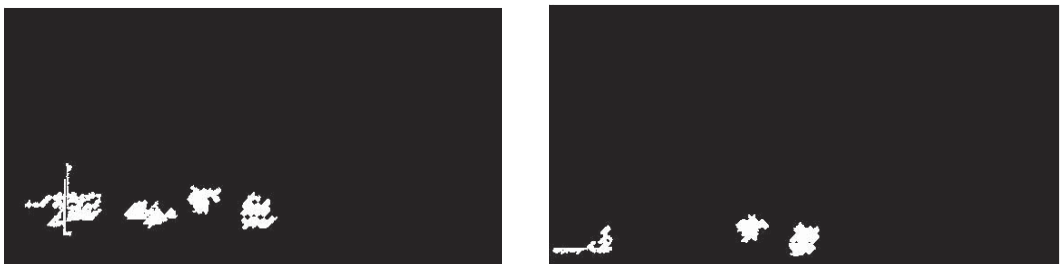

(a) (b)

(c)

Fig. 10.29 The CHM1_II-2 (a), CHM1_II-6 (b) and CHM1_II-10 (c)

(a)

(b)

(c)

Fig. 10.30 The CHM1_II-3 (a), CHM1_II-7 (b) and CHM1_II-11 (c)

(a)

(b)

(c)

Fig. 10.31 The CHM1_II-4 (a), CHM1_II-8 (b) and CHM1_II-12 (c)

As seen in Figs. 10.28, 10.29, 11.30 and 11.31, disappearing of an intruder and appearing of a school bag behind fence wires have been detected by the first algorithm. The intruder has been detected undersegmentation as a consequence of background clutter of the third outdoor scene. The Zitnick and Kanade algorithm fails to detect a half part of the intruder's occlusion regions since background behind the intruder and a half part of the intruder, from the middle to the top, are in darker regions. However, several false positives have been detected by the first algorithm as well.

The following Figs. depict changed masks produced by the second algorithm.

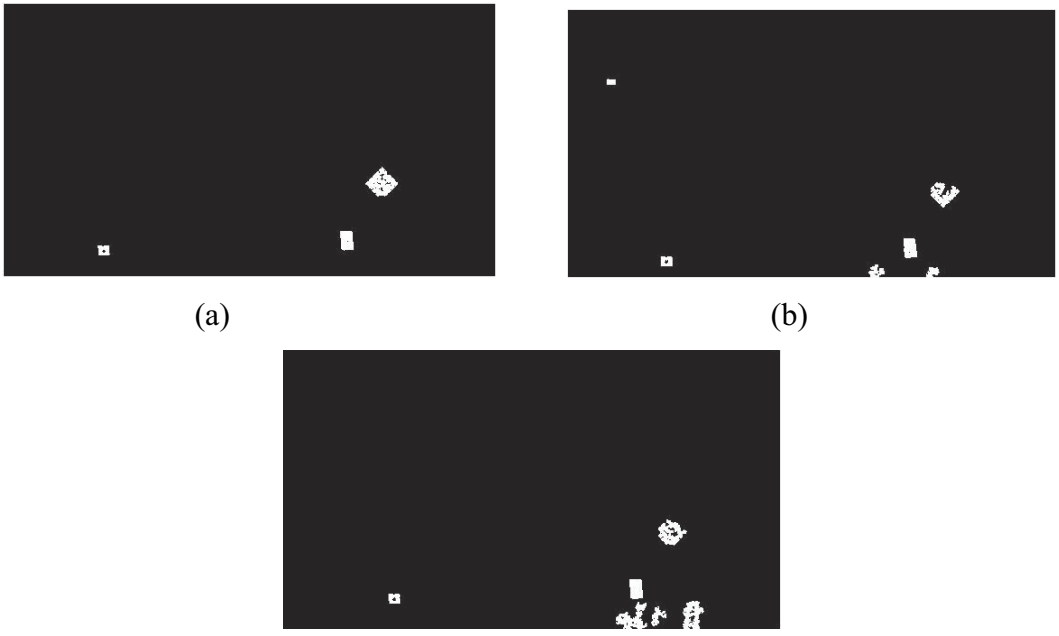

(a) (b)

(c)

Fig. 10.32 The CHM2_II-1 (a), CHM2_II-5 (b) and CHM2_II-9 (c)

(a) (b)

(c)

Fig. 10.33 The CHM2_II-2 (a), CHM2_II-6 (b) and CHM2_II-10 (c)

(a)

(b)

(c)

Fig. 10.34 The CHM2_II-3 (a), CHM2_II-7 (b) and CHM2_II-11 (c)

(a)

(b)

(c)

Fig. 10.35 The CHM2_II-4 (a), CHM2_II-8 (b) and CHM2_II-12 (c)

As seen in Figs. 10.32, 10.33, 10.34 and 10.35, a breach and two attached objects have been detected by the second algorithm. However, several unimportant changes have been detected by the second algorithm as well. The unimportant changes are very complicated to be prevented since they are often close enough to size and contour of the significant changes.

10.2.3.3 Locations of Changes

The following Figs. depict estimated locations and possible percentages of significant changes on registered input images.

(a)

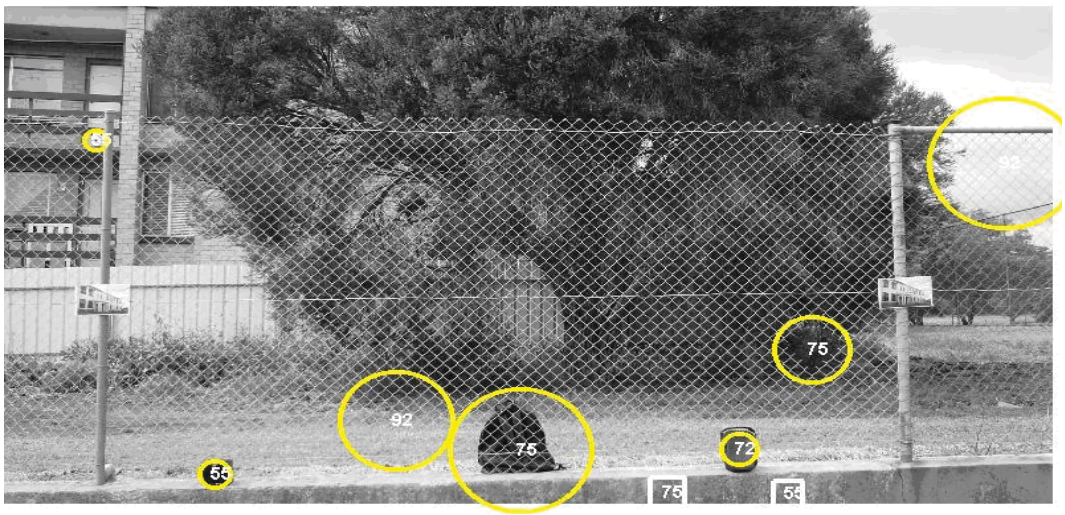

(b)

(c)

Fig. 10.36 Estimated locations and possible percentages of significant changes provided by the outdoor change detection method from the ROI2_II-1 (a), ROI2_II-5 (b) and ROI2_II-9 (c)

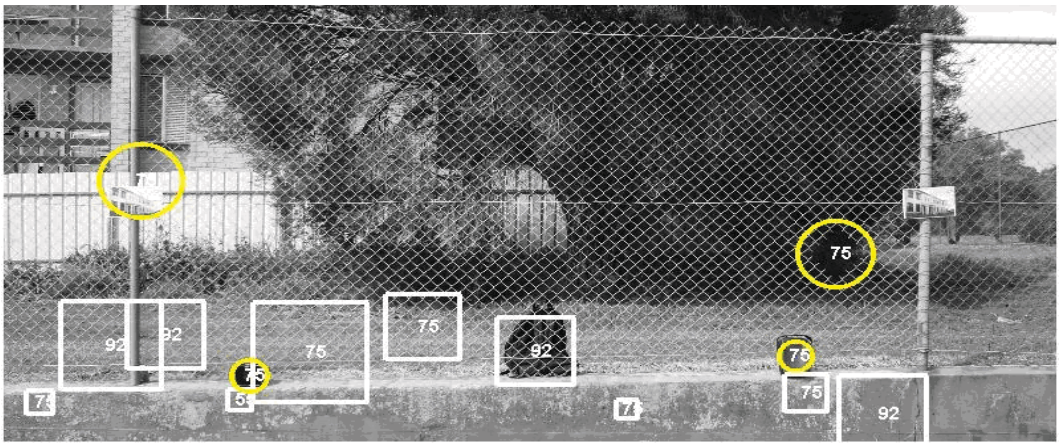

(a)

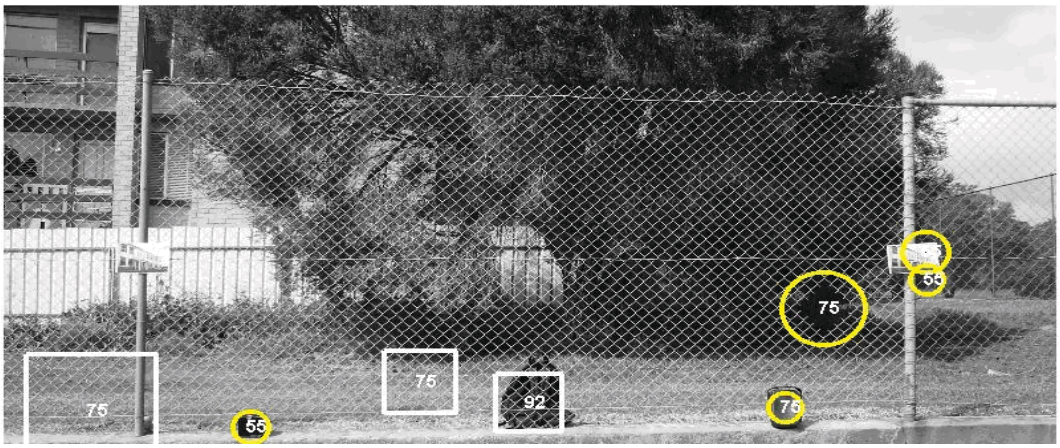

(b)

(c)

Fig. 10.37 Estimated locations and possible percentages of significant changes provided by the outdoor change detection method from the ROI2_II-2 (a), ROI2_II-6 (b) and ROI2_II-10 (c)

(a)

(b)

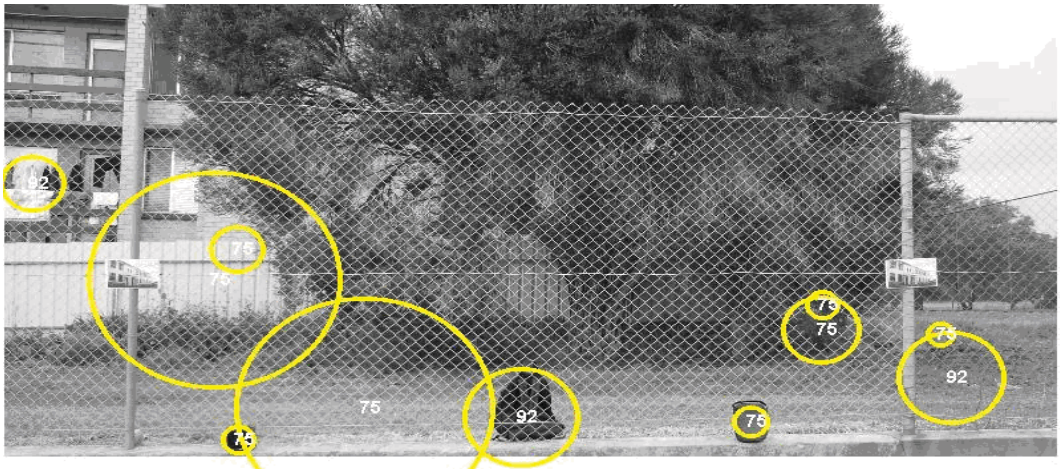

(c)

Fig. 10.38 Estimated locations and possible percentages of significant changes provided by the outdoor change detection method from the ROI2_II-3 (a), ROI2_II-7 (b) and ROI2_II-11 (c)

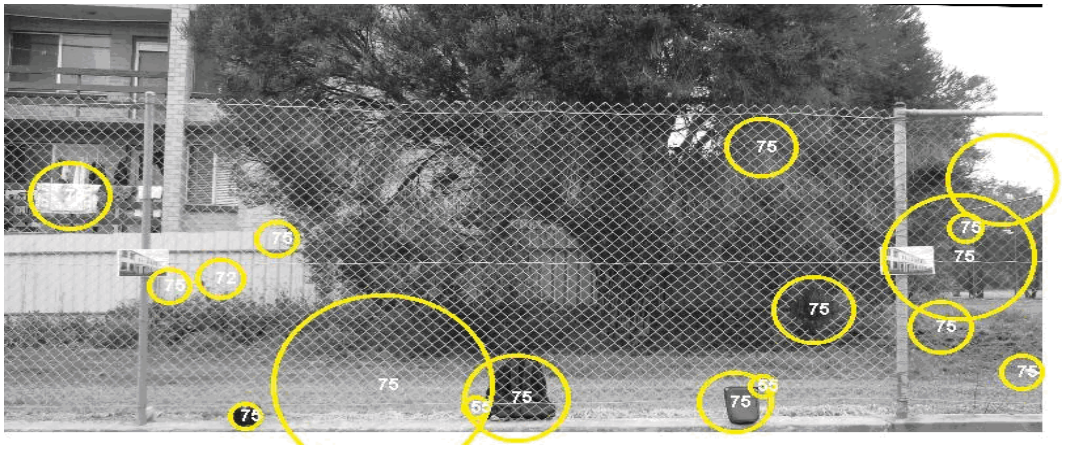

(a)

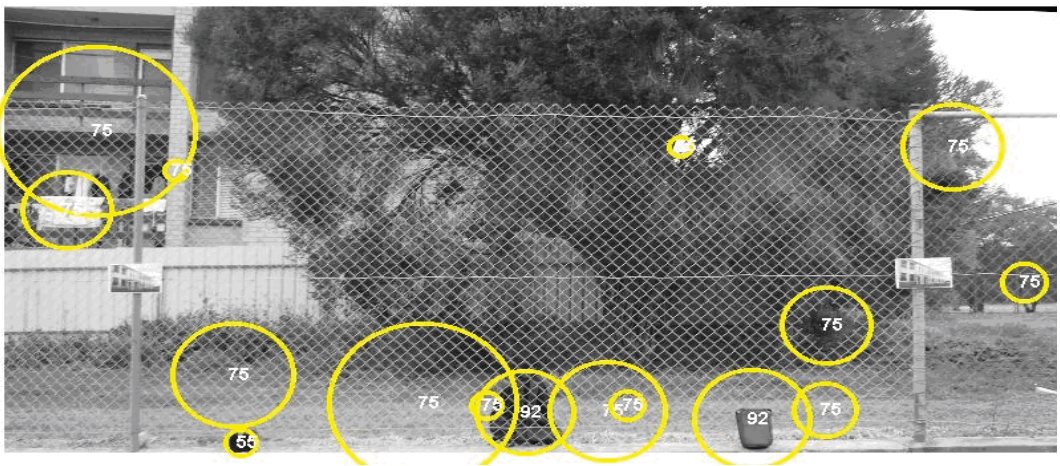

(b)

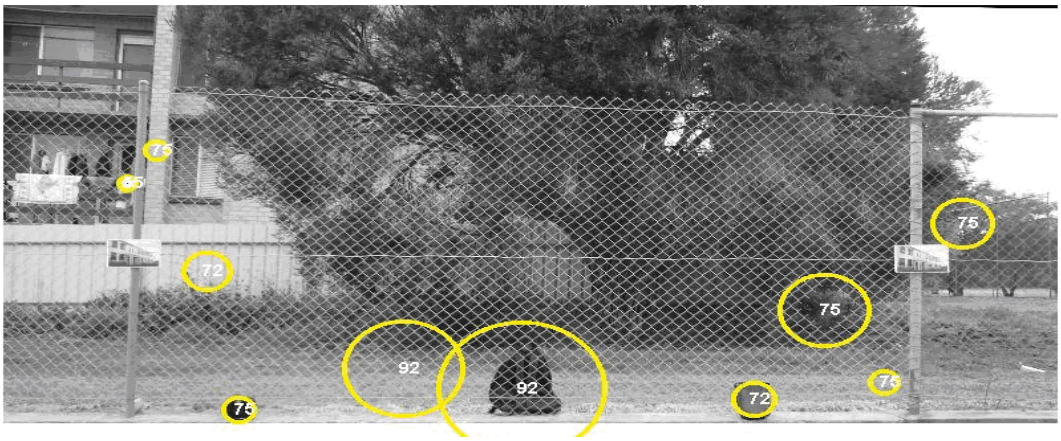

(c)

Fig. 10.39 Estimated locations and possible percentages of significant changes provided by the outdoor change detection method from the ROI2_II-4 (a), ROI2_II-8 (b) and ROI2_II-12 (c)

As seen in Figs. 10.36, 10.37, 10.38 and 10.39, all significant changes such as appearing and disappearing of a school bag and an intruder behind fence wires, two attached objects in front of fence wires and a medium breach in the integrity of fence wires have been detected and located correctly by the outdoor change detection method. Possible percentages of these significant changes are in the range of 55 – 92. At the same time, the outdoor change detection method has also detected several unimportant changes.

10.3 Discussion

The main purpose of the presented outdoor change detection method is to provide assistance to operators in an inspection room regarding regions of change in multiple outdoor images of the same scene containing fence wires acquired by a mobile camera from slightly different viewing positions, angles and at different times by displaying anticipated locations of and possible percentage values of significant changes in each input image. Regions of change are presented in white square and yellow circle forms in order to attract the attention of operators in the monitor room for a further investigation.

The change detection method tries to detect estimated locations of potential significant changes in each input image since it is quite complicated to detect exact locations of significant changes in these kinds of multiple outdoor images

because of camera movement, sensor noise, illumination variation, background clutter, and tiny sizes of fence wires. At the end, human operators in an inspection room will determine the final decision whether or not there are real significant changes in each input image by referring to change detection results produced by the change detection method.

In evaluating the performance of the outdoor change detection method, the subjective quality evaluation by human observers, quantitative evaluation by the ground truth measure (i.e., pixel-based measure), and computational time consumption are used in this study. Moreover, the effect of camera movement and rotation restrictions on the performance of the change detection method is discussed. Finally, the effect of object shadows on the performance of the method is provided. The followings are results of assessing and discussing the performance of the change detection method.

10.3.1 Subjective Quality Evaluation

In this sub-section, detection results produced by the outdoor change detection method from multiple outdoor images of the same scene captured by a mobile camera from the first and second outdoor scenes are assessed using the subjective quality evaluation by human observers.

10.3.1.1 First Outdoor Scene

There are six significant changes – a school bag disappearing behind fence wires, an intruder appearing behind fence wires, two attached objects in front of fence wires, large and small breaches in the integrity of fence wires – that must be able to detect and locate by the change detection method from multiple outdoor images of the same scene containing fence wires taken by a mobile camera from the first outdoor scene. As depicted in Figs. in sub-section 10.2.1 above, the outdoor change detection method detects all significant changes, true positives (correctly detected as foreground). There are a few same regions, especially the intruder and large breach regions, detected two to three times. It happens because the regions are detected in the first and second algorithms, respectively. Table 10.5 summarizes the detecting results.

Table 10.5 Summarization of detection results produced by the outdoor change detection method towards multiple outdoor images of the same scene taken from the first outdoor scene

Input Image	TP	FN	FP
1	6	-	3
5	6	-	2
9	6	-	2
2	6	-	5
6	6	-	5
10	6	-	-
3	6	-	2
7	6	-	2
11	6	-	7
4	6	-	3
8	6	-	1
12	6	-	-
Total	72	-	32

where TP stands for true positive, correctly detected as foreground, FN is false negative (miss), falsely detected as background, and FP is false positive (false alarm), falsely marked as foreground.

The true positive rate (*TPR*) and the false negative rate (*FNR*) are determined by referring to (10.1) and (10.2), below.

$$TPR = TP \;/\; (TP + FN) \tag{10.1}$$

$$FNR = FN \;/\; (TP + FN) \tag{10.2}$$

The *TPR* and *FNR* of the change detection method are 100.00 % and 0.00 %.

Although the change detection method detects all significant changes in the multiple outdoor images, it also detects several false positives (FP or false alarm), falsely marked as foreground, of which the mainly occur in the ROI2_II-2, ROI2_II-6 and ROI2_II-11 (see Figs. 10.2 (a), 10.2 (b) and 10.3 (c), above).

10.3.1.2 Second Outdoor Scene

There are six significant changes, disappearing and appearing of a school bag and an intruder, two attached objects in front of fence wires and two medium and

small breaches in the integrity of fence wires, that must be able to be detected by the outdoor change detection method from new multiple images of the same scene captured by a mobile camera from the second outdoor scene. Referring to Figs. in sub-section 10.2.2.3, all significant changes have been detected by the outdoor change detection method while several unimportant changes have been detected as well. Table 10.6 summarizes detection results of new input images produced by the change detection method.

Table 10.6 Summarization of detection results produced by the outdoor change detection method after applying new multiple outdoor images of the same scene taken from the second outdoor scene

Input Image	TP	FN	FP
1	6	-	-
5	6	-	3
9	6	-	1
2	6	-	3
6	6	-	4
10	6	-	2
3	6	-	5
7	6	-	5
11	6	-	3
4	6	-	4
8	6	-	7
12	6	-	-
Total	72	-	37

The true positive rate (*TPR*) and the false negative rate (*FNR*) are determined by referring to (10.1) and (10.2), above, are 100.00 % and 0.00 %. However, the change detection method also detects several false positives (FP or false alarm) depicted in Figs. 10.19 (b), 10.20 (a) – (b), 10.21 (a) – (b) and 10.22 (a) – (b), above.

10.3.1.3 Third Outdoor Scene

There are five significant changes, disappearing and appearing of an intruder and a school bag, two attached objects in front of fence wires and a medium breach in the integrity of fence wires, that must be able to be detected by the outdoor change

detection method from new multiple images of the same scene captured by a mobile camera from the third outdoor scene. Referring to Figs. in sub-section 10.2.2.3, all significant changes have been detected by the outdoor change detection method while several unimportant changes have been detected as well. Table 10.7 summarizes detection results of new input images produced by the change detection method.

Table 10.7 Summarization of detection results produced by the outdoor change detection method after applying new multiple outdoor images of the same scene taken from the third outdoor scene

Input Image	TP	FN	FP
1	5	-	-
5	5	-	4
9	5	-	3
2	5	-	9
6	5	-	3
10	5	-	3
3	5	-	9
7	5	-	3
11	5	-	5
4	5	-	12
8	5	-	11
12	5	-	5
Total	60	-	57

The true positive rate (*TPR*) and the false negative rate (*FNR*) are determined by referring to (10.1) and (10.2), above, are 100.00 % and 0.00 %. However, the change detection method also detects numerous false positives (FP or false alarm).

10.3.2 Quantitative Evaluation

In this sub-section, detection results produced by the outdoor change detection method from multiple outdoor images of the same scene captured by a mobile camera from the first and second outdoor scenes are assessed using the ground truth measure.

10.3.2.1 First Outdoor Scene

The ground truth measure is a pixel-based measure. A ground truth (i.e., an expected changed mask) is needed in the ground truth approach. Fig. 10.40 below depicts a ground truth used to all multiple outdoor images captured from the first outdoor scene.

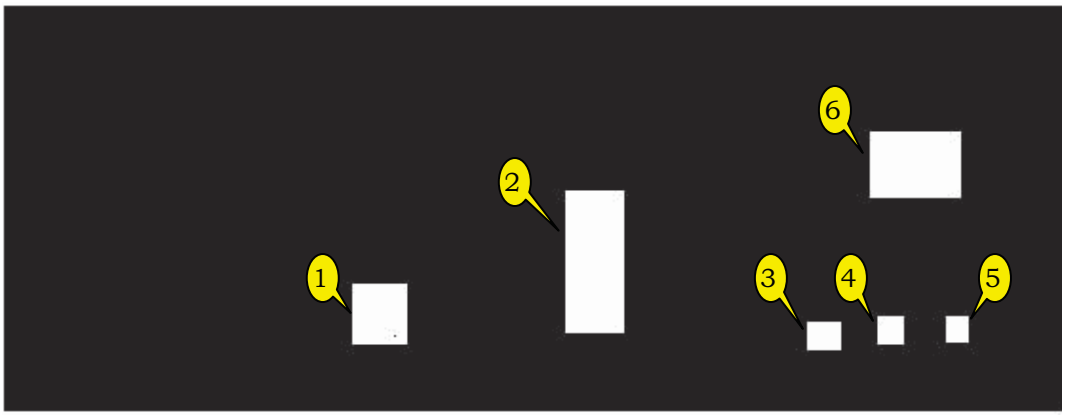

Fig. 10.40 A ground truth image extracted from the multiple outdoor images of the first outdoor scene used to asses the performance of the change detection method

As depicted in Fig. 10.40, there are six significant changes in the multiple outdoor images. Table 10.8 summarizes areas of objects (Kbytes) in the ground truth image.

Table 10.8 Summarization of object areas in Kbytes extracted from the ground truth image in Fig. 10.40 above

Object	Label	Ground Truth Area (Kbytes)
1	School Bag	28.81
2	Intruder	72.12
3	First Box	8.47
4	Second Box	6.64
5	Small Breach	5.31
6	Large Breach	52.21

As depicted in Table 10.8 above, the intruder is the bigger object in the ground truth image and the small breach is the smallest object. The large breach has a size

more than ten times than the small breach size. Moreover, the first box is bigger than the second box.

Next, for every object in every changed mask, its area is compared with its ground truth area. If its area in the changed mask is smaller than its ground truth area, then the object has suffered from false negatives (FN). If its area in the changed mask is bigger than its ground truth area, then the object has suffered from false positives (FP). Table 10.9 below depicts a set of TP, FN, FP and TN (i.e., true negative, correctly detected as background) numbers produced by the ground truth measure.

Table 10.9 Summarization of TP, FN, FP and TN numbers in Kbytes

Input Images	TP (Kbytes)	FN (Kbytes)	FP (Kbytes)	TN (Kbytes)
1	115.70	57.86	35.85	3435.82
5	140.36	33.20	31.49	3440.18
9	98.39	74.90	23.78	3448.16
2	113.47	60.08	46.60	3425.07
6	138.86	34.70	64.76	3406.91
10	120.58	52.98	8.54	3463.13
3	136.91	36.65	14.24	3457.43
7	108.29	65.27	36.38	3435.29
11	112.67	60.89	193.84	3277.83
4	114.81	58.75	16.89	3454.79
8	144.00	29.56	33.25	3438.42
12	140.09	33.47	3.32	3468.35
Total	1484.13	598.32	508.94	41151.38

Referring to equations (10.1) and (10.2) above, the *TPR* and *FNR* of the change detection are 71.27 % and 28.73 %. The false positive rate (*FPR*) and true negative rate (*TNR*) are calculated by referring to equations (10.3) and (10.4) below.

$$TNR = TN \;/\; (TN + FP) \tag{10.3}$$

$$FPR = FP \;/\; (TN + FP) \tag{10.4}$$

The *TNR* and *FPR* of the change detection method are 98.78 % and 1.22 %.

Furthermore, the recall, R, is calculated referring to equation (10.5) below. The R is the ratio between the number of correctly detected pixels to the number of relevant pixels in the ground truth data. The R is used to estimate the tendency of undersegmentation, large number of false negatives.

$$R = TP / (TP + FP) \tag{10.5}$$

The R value of the change detection method is 74.46 %. The higher the R the less likely is undersegmentation.

Next, the precision, P, is calculated referring to equation (10.6) below. The P is the ratio between the number of correctly detected pixels to the total number of pixels. The P is used to analyse the tendency of a change detection method to oversegmentation, large number of false positives.

$$P = TP / (TP + FN) \tag{10.6}$$

The P value of the change detection method is 71.27 %. The higher the P the less likely is oversegmentation.

Finally, the F_measure combines these complementary measures with equal weights by referring to equation (10.7) below.

$$F = 2.P.R / (P + R) \tag{10.7}$$

The F is an overall criteria of the segmentation quality and the F value of the change detection method is 72.83 %.

Based on information of the *TPR*, *FNR*, *TNR, FPR*, R, P and F values, the presented change detection method has a good capability to detect correctly all significant changes in multiple outdoor images of the same scene captured by from the first outdoor scene by a mobile camera. However, the presented method has to improve since the method misses a lot of true positives. Although the method fails to spot lots of corrected pixels, the method can minimize unimportant changes in these kinds of multiple outdoor images. Overall, the

method can detect correctly any potential significant changes such as appearing and disappearing of objects behind fence wires, breaches in the integrity of and attached objects in front of fence wires while minimizing unimportant changes caused mainly by camera motion, illumination variation, background clutter, tiny sizes of fence wires and non-uniform illumination that occurs across fence wires.

10.3.2.2 Second Outdoor Scene

Fig. 10.41, below, depicts a ground truth image used by the ground truth measure in evaluating the performance of the outdoor change detection method in processing new images captured from the second outdoor scene.

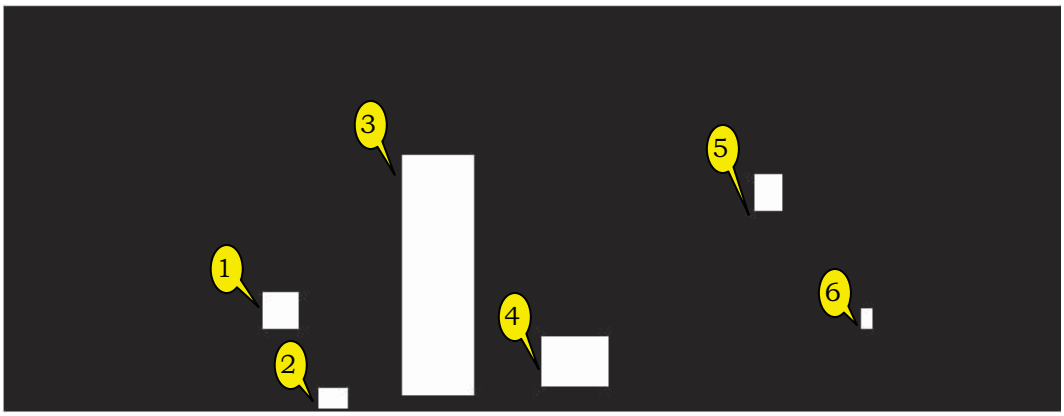

Fig. 10.41 A ground truth image extracted from new images captured from the second outdoor scene used to evaluate the performance of the change detection method

Table 10.10 summarizes areas of objects (Kbytes) in the ground truth image in Fig. 10.41, above.

Table 10.10 Summarization of object areas in Kbytes extracted from the ground truth image in Fig. 10.41 above

Object	Label	Ground Truth Area (Kbytes)
1	Medium Breach	16.60
2	Small Box	7.01
3	Intruder	222.09
4	School Bag	43.31
5	Small Bag	13.22
6	Small Breach	2.89

As depicted in Table 10.10 above, the intruder is the bigger object in the ground truth image and the small breach is the smallest object. The medium breach has a size around eight times than the small breach size. Moreover, the school bag is the second bigger after the intruder in the ground truth image. The small bag is around two times bigger than the small box.

Table 10.11 summarizes a set of TP, FN, FP and TN values produced by the ground truth measure after comparing every object area in each changed mask with its ground truth area.

Table 10.11 Summarization of TP, FN, FP and TN values in Kbytes

Input Images	TP (Kbytes)	FN (Kbytes)	FP (Kbytes)	TN (Kbytes)
1	286.45	18.67	11.88	5142.26
5	298.19	6.93	54.06	5100.09
9	279.52	25.60	23.59	5130.56
2	289.00	16.12	17.20	5136.95
6	300.84	4.28	47.71	5106.44
10	294.91	10.21	18.82	5135.33
3	288.28	16.84	37.70	5116.44
7	301.29	3.83	38.82	5115.32
11	296.24	8.88	55.38	5098.77
4	279.70	25.42	38.41	5115.74
8	299.23	5.89	55.01	5099.14
12	258.12	47.00	6.22	5147.93
Total	3471.76	189.67	404.79	61444.98

Table 10.12 depicts *TPR*, *FNR*, *TNR, FPR*, R, P and F values of the outdoor change detection method referring to equations 10.1, 10.2, 10.3, 10.4, 10.5, 10.6 and 10.7 above.

Table 10.12 *TPR*, *FNR*, *TNR, FPR*, R, P and F values of the outdoor change detection method produced by the ground truth measure

Parameter	Values (%)
TPR	94.82
FNR	5.18
TNR	99.35
FPR	0.65
R	89.56
P	94.82
F	92.11

As depicted in Table 10.12, *TPR* and *FNR* of the change detection method are 94.82 % and 5.18 %. These percentages indicate that the change detection method can correctly detect all significant changes and it only misses a small amount of true positive pixels. *TNR* and *FPR* of the change detection method are 99.35 % and 0.65 %. These two percentages indicate that the change detection method only suffers a small amount of false positives. R and P values indicate that the change detection method is not undersegmentation or oversegmentation. Overall, the segmentation quality of the change detection method in processing new multiple images of the same scene captured by a mobile camera from the second outdoor scene is acceptable and good indicated by its F value, 92.11 %.

10.3.2.3 Third Outdoor Scene

Fig. 10.42, below, depicts a ground truth image used by the ground truth measure in evaluating the performance of the outdoor change detection method in processing new images captured from the third outdoor scene.

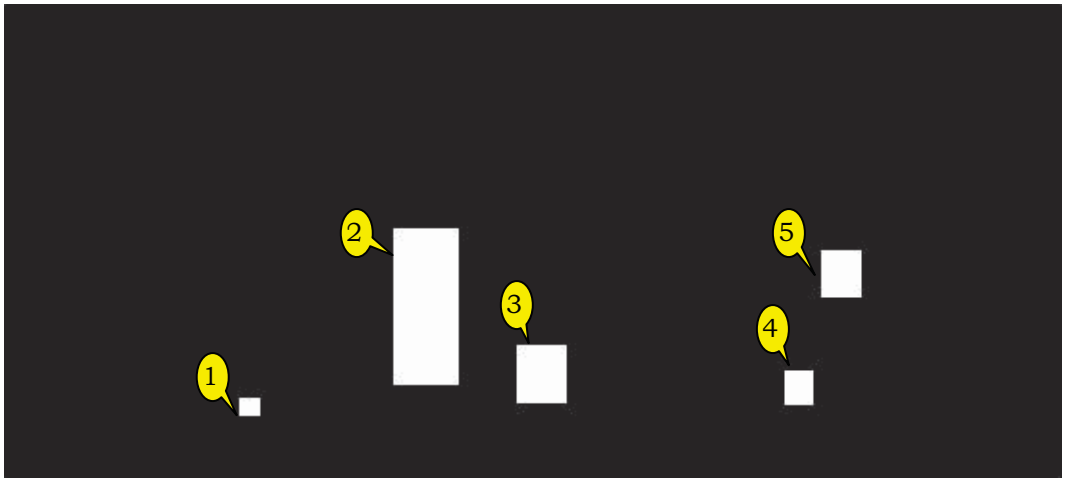

Fig. 10.42 A ground truth image extracted from new images captured from the third outdoor scene used to evaluate the performance of the change detection method

Table 10.13 summarizes areas of objects (Kbytes) in the ground truth image in Fig. 10.42, above.

Table 10.13 Summarization of object areas in Kbytes extracted from the ground truth image in Fig. 10.42 above

Object	Label	Ground Truth Area (Kbytes)
1	Small Box	3.45
2	Intruder	60.52
3	School Bag	25.10
4	Small Bag	9.07
5	Medium Breach	17.20

As depicted in Table 10.13 above, the intruder is the bigger object in the ground truth image and the small box is the smallest object. Moreover, the school bag is the second bigger after the intruder in the ground truth image. The small bag is around two times bigger than the small box.

Table 10.14 summarizes a set of TP, FN, FP and TN values produced by the ground truth measure after comparing every object area in each changed mask with its ground truth area.

Table 10.14 Summarization of TP, FN, FP and TN values in Kbytes

Input Images	TP (Kbytes)	FN (Kbytes)	FP (Kbytes)	TN (Kbytes)
1	86.58	28.75	12.73	4284.10
5	83.52	31.81	39.36	4257.47
9	77.47	37.87	72.77	4224.06
2	72.92	42.41	142.35	4154.48
6	71.89	43.45	28.52	4268.32
10	72.85	42.48	38.69	4258.14
3	64.20	51.14	142.70	4154.13
7	76.13	39.21	65.53	4231.30
11	111.87	3.47	117.06	4179.78
4	113.91	1.42	119.18	4177.66
8	95.29	20.04	129.04	4167.79
12	73.14	42.19	28.17	4268.67
Total	999.79	384.24	936.10	50625.89

Table 10.15 depicts *TPR*, *FNR*, *TNR, FPR*, R, P and F values of the outdoor change detection method referring to equations 10.1, 10.2, 10.3, 10.4, 10.5, 10.6 and 10.7 above.

Table 10.15 *TPR*, *FNR*, *TNR, FPR*, R, P and F values of the outdoor change detection method produced by the ground truth measure

Parameter	Values (%)
TPR	72.24
FNR	27.76
TNR	98.18
FPR	1.82
R	51.64
P	72.24
F	60.23

As depicted in Table 10.15, *TPR* and *FNR* of the change detection method are 72.24 % and 27.76 %. These percentages indicate that the change detection method misses 27.76 % of all true positive pixels especially a quarter part of the intruder since background behind the intruder and the intruder it self are in darker regions. *TNR* and *FPR* of the change detection method are 98.18 % and 1.82 %. These two percentages indicate that the change detection method suffers a small amount of false positives. The R value, 51.64 %, indicates that the change detection method suffers from undersegmentation especially the intruder. The P value, 72.24 %, indicates that the change detection method is a little bit oversegmentation since it detects several false positives as well. Overall, the segmentation quality of the change detection method in processing new multiple images of the same scene captured by a mobile camera from the third outdoor scene is in an above average indicated by its F value, 60.23 %.

10.3.3 Computational Time Consumption

In this sub-section, computational time consumptions used the outdoor change detection method to produce detection results of multiple outdoor images of the same scene captured by a mobile camera from the first, second and third outdoor scenes are presented.

10.3.3.1 First Outdoor Scene

For the computational complexity evaluation, all input images were processed in a computer laptop with specifications as follows. Its hardware is Toshiba Tecra A3,

Intel Pentium M 1.6 GHz and 760 MB of RAM. Its software is Windows XP Professional Version 2002, Service Pack 1 and the program was run in the Matlab environment. Time consumptions needed by the computer to process all input images are depicted in Table 10.16, below.

Table 10.16 Time consumptions needed the computer to process each input image

Input Image	ZKA (minutes)	Detection (minutes)	Total (minutes)
1	22	5.36	27.36
5	23	5.36	28.73
9	24	5.36	29.88
2	26	5.36	31.83
6	26	5.36	32.9
10	26	5.36	33.52
3	27	5.36	33.73
7	28	5.36	34.89
11	31	5.36	40.19
4	27	5.36	33.88
8	23	5.36	28.38
12	24	5.36	29.63
Total	307	77.92	384.92

As depicted in Table 10.16 above, the ZKA is a time needed by the Zitnick and Kanade algorithm to produce a confidence map image. Since the Zitnick and Kanade algorithm is a stereo computational algorithm and the file size of an input image used in this research is an 8Mbytes, the Zitnick and Kanade algorithm uses almost 80.41 % of the total time for each input image. The detection time means a time needed by the change detection method to process the confidence map image in producing an occlusion map image and detecting significant changes from the occlusion map image. The adaptive thresholding technique uses almost 50 % of the detection time for each input image in generating a binary image from an edged image. The reason of using an 8Mbytes image in this research is to provide enough pixel information of fence wires to 2 – 3 pixels since the distance between the digital camera and the wire fence is 6 meters when capturing input images. Since the research is an initial study of change detection methods for multiple outdoor images of the same scene containing fence wires captured by a mobile

camera from slightly different viewing positions, angles and at different times, the computational time consumption is not a major concern. Hopefully, the computer hardware will improve significantly in terms of speed and capacity in the future and the computational time consumption can be overcome respectively.

10.3.3.2 Second Outdoor Scene

Table 10.17 depicts time consumptions used the computer to process new multiple outdoor images taken from the second outdoor scene.

Table 10.17 Time consumptions needed the computer to process new images captured from the second outdoor scene

Input Image	ZKA (minutes)	Detection (minutes)	Total (minutes)
1	44	11.23	55.23
5	43	9.84	52.84
9	40	9.67	49.67
2	37	8.98	45.98
6	45	11.06	56.06
10	41	9.95	50.95
3	41	10.63	51.63
7	42	10.83	52.83
11	41	12.48	53.48
4	39	8.93	47.93
8	37	9.27	46.27
12	40	9.29	49.29
Total	490	122.16	612.16

As depicted in Table 10.17, the Zitnick and Kanade algorithm uses almost 80 % of the total time. To generate changed masks from the confidence map images produced by the Zitnick and Kanade algorithm, the computer uses around 20 % of the total time. The change detection method uses longer times in processing input images captured from the second outdoor scene rather than in processing input images captured from the first outdoor scene since file sizes of input images captured from the second outdoor scene are bigger than file sizes of input images captured from the first outdoor scene. These different file sizes occur as a result of extraction automatically regions of interest from registered input images.

10.3.3.3 Third Outdoor Scene

Table 10.18 depicts time consumptions used the computer to process new multiple outdoor images taken from the third outdoor scene.

Table 10.18 Time consumptions needed the computer to process new images captured from the third outdoor scene

Input Image	ZKA (minutes)	Detection (minutes)	Total (minutes)
1	33	8.55	41.55
5	33	7.99	40.99
9	36	9.49	45.49
2	27	6.94	33.94
6	32	6.85	38.85
10	26	5.70	31.7
3	33	9.56	42.56
7	30	7.32	37.32
11	32	7.80	39.8
4	33	8.75	41.75
8	34	8.53	42.53
12	35	7.06	42.06
Total	384	94.54	478.54

As depicted in Table 10.18, the Zitnick and Kanade algorithm uses almost 80 % of the total time. To generate changed masks from the confidence map images produced by the Zitnick and Kanade algorithm, the computer uses around 20 % of the total time.

10.3.4 The Effect of Camera Movement and Rotation Restrictions on the Performance of the Method

An assumption, restrictions of the camera movement in both X and Y axes and the camera rotation in $\Delta\theta_z$ axis, is applied into the outdoor change detection method in this research in order to simulate patrol robot navigation errors caused mainly by patrol robot sensors such as GPS, compass and accelerometer accuracies. The distance of movement in X and Y axes was restricted in a range of ± 20 cm, and the rotation of $\Delta\theta_z$ axis was limited in a range of ± 15 degrees.

Since the first algorithm of the outdoor change detection method uses human-made templates attached on left and right posts of the wire fence as sources of control points for image registration, left and right posts of the wire fence are crucial and must appear in all input images. When either left post or right post misses within an input image, the first algorithm of the method will fail to perform further process to the input image. The following negative impact to the method is that the second algorithm of the method will fail as well since input images, ROI2_IIs, used by the second algorithm are provided by image registration. Therefore, restrictions of camera movement in both X and Y axes and rotation in $\Delta\theta_z$ axis will ensure that left and right posts of the wire fence always emerge in every input image otherwise the method will be unsuccessful to process the input image. In other words, as long as left and right posts of the wire fence appear within an input image, it doesn't matter from which positions and angles that the input image is captured, the method will be able to detect regions of change while reducing unimportant changes in the input image.

In the real-time application, outdoor environment provides different kinds of terrain conditions all the time. Hence, camera movement in Z axis (i.e., vertical movement) cannot be prevented when a camera is mounted on a mobile robot. As a result, heights of camera positions may vary when capturing input images. Consequently, bottom and top of scenes in input images may differ. Since searching of regions of change is limited from the ground to 1.5 m height, vertical movement of the camera may not significantly effect the performance of the outdoor change detection method as long as left and right posts of the wire fence emerge within input images.

10.3.5 The Effect of Object Shadows on the Performance of the Method

Shadows of the intruder and fence posts can be seen in the reference image and all input images of the second outdoor scene in Chapter 10 (i.e., Fig. 10.5, Figs. 10.6 (a) – (c), Figs. 10.7 (a) – (c), Figs. 10.8 (a) – (c) and Figs. 10.9 (a) – (c)). Moreover, a shadow of the intruder appears in the reference image of the third outdoor scene (i.e., Fig. 10.23).

Although the outdoor change detection method has been successful in detecting significant changes in all input images, the method, especially the first algorithm, often suffers from the effect of object shadows. Fortunately, shadows of fence posts can be minimized by image registration since shadows of fence posts often appear on the grass in front of the wire fence. After performing image registration towards the reference and input images based on CPs extracted from reference and input images, the grass in front of the wire fence is often cropped automatically. On the other hand, the intruder's shadow is quite hard to be avoided; as a result, the method tends to detect it as a part of the intruder shown in Figs. 10.11 (a) – (c), Figs. 10.30 (a) – (b), Figs. 10.31 (a) – (b).

10.4 Concluding Remarks

Prior to depict estimated locations and possible percentage values of significant changes on each ROI2_II, latest possible percentage values of objects in each changed mask produced by the first and second algorithms have to be calculated again since possible percentage values generated by the FIS1 and FIS2 tend to be the same. Thus, the FIS3 is developed in this research. The range of possible percentage values produced by the FIS3 is a range of 49 – 100. The higher the possible percentage value the more likely that the region of change is a significant change.

Multiple outdoor images of the same scene containing fence wires captured by a mobile camera from two different outdoor scenes are used as input to the outdoor change detection method. The subjective evaluation by human observers, quantitative evaluation by the ground truth measure and computational time consumptions are used in this research in order to asses the performance of the outdoor change detection method. Overall, the outdoor change detection method can detect correctly any potential significant changes such as appearing and disappearing of objects behind fence wires, breaches in the integrity of and attached objects in front of fence wires in these kinds of multiple outdoor images while minimizing unimportant changes caused mainly by camera motion, illumination variation, background clutter, tiny sizes of fence wires and non-uniform illumination that occurs across fence wires. Moreover, in the case

quantitative evaluation by the ground truth measure, when R and P values are less than 55 %, then the method has suffered from both undersegmentation and oversegmentation.

Since the research is an initial study in change detection methods for multiple outdoor images of the same scene containing fence wires acquired by a mobile camera from slightly different viewing positions, angles and at different times, the computational complexity, time consumptions needed by the computer to process input images, is not a major concern in this research. In the future, when the computer hardware has significantly improved in terms of speed and capacity, the computational complexity will be able to overcome respectively. Moreover, the first and second algorithms can also be further researched in order to reduce the computational time.

CHAPTER 11

CONCLUSIONS AND FUTURE WORK

In this chapter, conclusions of the research are presented in Section 11.1 and a summary of main contributions is described in Section 11.2. Finally, recommendations for future work are provided in Section 11.3.

11.1 Conclusions of the Research

The research is the first attempt in developing an automated change detection method for multiple outdoor images of the same scene containing fence wires captured by a mobile camera from slightly different viewing positions, angles and at different times. In perceiving an initial solution on how to minimize parallax in multiple images of the same scene taken by a mobile camera, an initial study was performed a simple indoor environment. The simple indoor change detection method is utilized in detecting regions of change in multiple images of a same indoor scene captured by a mobile camera from slightly different viewing positions and angles. Illumination variation has not put into consideration yet. The indoor change detection method consists of three main stages: (1) automatic image registration, (2) temporal differencing and (3) unimportant changes removal.

Conclusions drawn from the preliminary study are used as an additional knowledge in developing an automated outdoor image change method. An outdoor scene that contains a diamond wire netting fence was chosen as an experimental environment. The reason of choosing this outdoor scene which contains a chain-link mesh fence is that chain-link fences are often used as physical barriers in low and medium protective areas such as airfields and perimeter surveillance of defence bases. Furthermore, multiple outdoor images of

the same scene were captured from the outdoor scene by a mobile camera from somewhat dissimilar viewing positions, angles and at dissimilar times.

The automated outdoor change detection method must be able to detect and display approximate locations and possible percentage values of three kinds of significant changes in these kinds of multiple outdoor images such as absence and presence of objects behind fence wires, breaches in the integrity of fence wires and attached objects in front of fence wires. At the same time, the outdoor change detection method must be able to reduce unimportant changes in these kinds of multiple outdoor images caused mainly by camera motion, illumination variation, sensor noise, background clutter, thinness of fence wires and non-uniform illumination that occurs across fence wires. In building the outdoor change detection method, two distinctive algorithms were developed in this research. The first algorithm is only used to detect absence and presence of objects behind fence wires and the second algorithm is only utilized to detect breaches in the integrity of and attached objects in front of fence wires. The reason of separating these algorithms is because both algorithms work in two completely different approaches.

The first algorithm consists of five stages. In the first stage, a current input image and the reference image are automatically registered. Prior to register both input and reference images, distinctive correspondence points are automatically extracted from both input and reference images by using a template-based matching approach. Two same building pictures were used as artificial templates attached on left and right posts of the fence and the SIFT operator was chosen as a local features extractor in this research. Output of the template-based matching approach is a couple of correspondence points extracted from both input and reference images. Based on information of correspondence points extracted in the previous process, the current input image was registered into a same coordinate system with the reference image. The linear conformal transformation was chosen in the research to transform the input image into a registered input image since there is no projection that occurs in the input image. However, there are two areas observably in the registered input image: a gray area with information on it and a black area with no information. Since the black area doesn’t contain information,

it has to be cropped from the registered input image. As a result of this black area cropping, size of the registered input image will decrease significantly. Since size of the registered input image must be same with size of the reference image for further process, the reference image must be cropped as well by using information used to crop the registered input mage. To extract automatically information used to crop the registered input and reference images, a region of interest extraction algorithm was developed in the research. Output of the registration process was two cropped registered input and reference images that have same sizes.

In the second stage, phenomena of zero, smaller and larger disparities and occluded regions that apparently appear in both cropped registered input and reference images leads on the investigation of stereo correspondence algorithms. As a result of the investigation, the Zitnick and Kanade algorithm was chosen in the research since this algorithm can explicitly detect occluded regions in two stereo images. Both cropped registered input and reference images are used as input into the Zitnick and Kanade algorithm. Output of the Zitnick and Kanade algorithm is a confidence map image. In the confidence map image, occluded regions are represented into darker regions and same objects are depicted into lighter regions. In this research, occluded regions are investigated further since occluded regions could become potential significant changes such as appearing and disappearing of objects.

In the third stage, occluded regions are automatically extracted from the confidence map image in generating an occlusion map image. After investigation of occluded region values in the confidence map image, occluded region values tend to have intensity values in between 39 and 40. An intensity histogram of occluded regions is created and values of 39 and 40 appear as the first and second peak values in the histogram. The brightness thresholding approach was performed to the confidence map image in which values of 39 and 40 were used as global threshold values. As a result of the brightness thresholding approach, an occlusion map image was generated and introduced in this research.

In the fourth stage, a first hybrid decision-making system is developed in deciding which occluded regions belong to significant or unimportant changes. It is possible since sizes and shapes of occluded regions that belong to significant

changes are quite different from sizes and shapes of occluded regions that belong to unimportant changes in the occlusion map image. Output of the first hybrid decision-making system is called as a HDS image.

In the fifth stage, false positives in the HDS image are reduced by using the template subtraction approach. Output of the template subtraction approach is the first changed mask that contains potential significant changes detected from both cropped registered input and reference images.

The second algorithm integrates four main steps. Prior to detect regions of change in fence wires, edges of fence wires must be detected first. To detect edges of fence wires, the Sobel edge detector was chosen in this research. Output of the Sobel detector is an edged image, which is normally in a gray level image. The edged image has often to be converted into a binary image for further process like boundary tracing. As a consequence of non-uniform illumination that occurs across fence wires, the global thresholding may not be the best solution in converting the edged image into a binary image. Thus, an adaptive thresholding technique was performed in this research in converting the gray level image into a binary image.

In the second step, edges of fence wires in the binary image were enhanced by using morphological operations such as dilation and erosion. As a result of enhancing, edges of fence wires apparently appear in the enhanced image.

In the third step, an area-based algorithm was developed in detecting breaches in the integrity of and attached objects in front of fence wires. The enhanced image was converted into a new binary image by performing brightness thresholding into it. Since the chain-link mesh fence is a diamond netting fence, objects in between edges of fence wires become diamond-shape objects in the new binary image. Unimportant changes can be separated from potential significant changes by removing diamond-shape objects. Diamond-shape objects were removed from the new binary image by eliminating objects that have sizes less than or equal to an average size of diamond-based objects. This process overcomes background clutter as well.

In the fourth step, a second hybrid decision-making system (HDS2) was developed in this research since sizes and shapes of objects produced by the

second algorithm are quite different with object sizes and shapes generated by the first algorithm. Output of the HDS2 was called the second changed mask.

In locating and displaying purposes, latest possible percentages as significant changes were calculated again. The third fuzzy inference system (FIS3) was developed in the research. Inputs for the FIS3 were important information of objects in both first and second changed masks such as sizes of objects in pixels, widths of objects in X and Y axes and absolute difference values of local features extracted by the SIFT operator in templates cropped from both cropped registered input and reference images. These possible percentages will vary from 49 to 100. Regions with higher percentages indicated that there were higher possible significant changes in the regions. Locations of significant changes were circled in two different colours as well: white and yellow colours. White circles indicated disappearing of old objects and yellow circles indicated appearing of new objects. Finally, latest possible percentages of and locations of significant changes were depicted in the cropped registered input image.

11.2 Summary of Main Contributions

The research presented in this dissertation has produced several contributions for the literature and future researchers. These contributions are summarized as follows including links to the appropriate section.

- The research has provided two new change detection methods for multiple images of a same scene captured by a mobile camera from slightly different viewing positions, angles and at different times. See sections 3.2, 7.2 and 9.2.

- The research has utilized occluded regions in a confidence map image generated by the Zitnick and Kanade algorithm as potential significant changes in order to detect regions of change in these kinds of multiple outdoor images. See sections 6.3 and 6.4.

- The research introduces an occlusion map image that contains occlusion regions extracted from a confidence map image generated by the Zitnick and

Kanade algorithm. Since the confidence map image is a gray image, the confidence map image is converted to a binary image by performing the brightness thresholding. The 39 and 40 global threshold values were experimentally determined and used in the brightness thresholding since occluded regions tend to fall into both threshold values. See sections 6.2, 6.3 and 6.4.

- Stereo correspondence algorithms (e.g., the Zitnick and Kanade algorithm) can be used to extract regions, which have zero and smaller disparity values, and to present them in a confidence map image. One of main advantages of the Zitnick and Kanade algorithm from other stereo correspondence algorithms is its ability to detect explicitly occluded regions in both left and right images captured by a stereo camera. In this study, the reference and registered input images are denoted as the left and right images. Moreover, the Zitnick and Kanade algorithm is used to detect regions whose disparity values from 0 to 8 in order to overcome considerable background clutter of an outdoor scene. See section 6.2.

- The Sobel edge detector combined with an adaptive thresholding technique is used to overcome the thinness of fence wires and non-uniform illumination that occurs across fence wires in order to detect edges of fence wires. See sections 8.2 and 8.3.

- The outdoor change detection includes fuzzy inference systems in building intelligent decision-making systems used to decide which objects belong to significant or unimportant changes. See sections 7.3, 9.2 and 10.1.

11.3 Recommendations for Future Work

As demonstrated in the experimental results section, the presented change detection method has been successful to detect and display estimated locations and possible percentages of significant changes. However, several unimportant changes observably appear as well. These unimportant changes are very difficult

to prevent because of complexity of these kinds of multiple outdoor images. In reducing unimportant changes, there are several different steps of development:

1. Further investigations in different kinds of image registration approaches are needed in solving parallax in multiple outdoor images of the same scene taken by a mobile camera since a linear-conformal approach based on information of two couple of correspondence points was used in this study. By adding more control points and using other image registration approaches could provide much better results in eliminating parallax in these kinds of multiple outdoor images.
2. Further investigations in other stereo correspondence algorithms can be conducted in finding better confidence map images since discovering correctly occluded regions in the confidence map images is a key step in detecting significant changes in these kinds of multiple outdoor images.
3. In detecting breaches in the integrity of fence wires, tracking and finding directly discontinuities on edges of fence wires are another possible solution that can be investigated further.

This study is an initial study in developing automated change detection methods for multiple outdoor images of the same scene acquired by a mobile camera from slightly different positions, angels and at different times. Results shown in this study are still far away from perfect since unimportant changes still observably appear. Thus, further investigations in new change detection methods for these kinds of multiple outdoor images are still far away from completed and this study can hopefully be as a base for further investigations in the future.

In this research, the outdoor change detection method is only tested in three outdoor scenes containing fence wires. When the method is applied in the real-time application by mounted a digital camera on a mobile robot, other challenging research works certainly arise including (1) Simultaneous localisation and image based change detection, (2) The movement of camera in vertical direction caused mainly by terrain changes and (3) Using natural templates instead of human-made templates for CPs extraction and change detection.